DMD Fast Forward. Published on June 9, 2022 as DOI: 10.1124/dmd.121.000825
This article has not been copyedited and formatted. The final version may differ from this version.

Title Page

Characterization of JNJ-2482272 [4-(4-methyl-2-(4-(trifluoromethyl)phenyl)thiazole-5-yl)pyrimidine-2-amine] as a Strong AhR Activator in Rat and Human

Kevin J. Coe, Mark Feinstein, J. William Higgins, Perry Leung, Brian P. Scott, Judy Skaptason, Yuen Tam, Laurie P. Volak, Jennifer Kinong, Anton Bittner, Heather McAllister, Nathan M. Lim, Michael Hack, and Tatiana Koudriakova

Affiliations

Janssen Research & Development, L.L.C., San Diego, CA (K.J.C., M.F., P.L., B.P.S., L.P.V., H.A., N.M.L., M.H., T.K.); Janssen Research & Development, L.L.C., San Francisco, CA (Y.T.), Neurocrine Biosciences, Inc, San Diego, CA (J.S.); Pfizer, San Diego, CA (J.K.); Turnstone Biologics, La Jolla, CA (A.B.); and Trestle Biotherapeutics, San Diego, CA (J.W.H.)

Running Title Page

Metabolism and AhR Activation of JNJ-2482272

Corresponding Author

Name: Kevin J. Coe

Address: Janssen Research & Development, L.L.C., 3210 Merryfield Row, San Diego, CA 92121-1126

Telephone: 858 784 3195

Fax Number: 858 784 3058

e-mail address: kcoe2@its.jnj.com

Number of text pages: 34

Number of tables: 6

Number of figures: 9

Number of references: 49

Number of words in abstract: 250

Number of words in introduction: 468

Number of words in discussion: 1479

Abbreviations used in this paper are:

3-MC, 3-methylcholanthrene; ABT, 1-amino-benzotriazole; AhR, aryl hydrocarbon receptor; AUC, area under the curve; βNF, β-naphthoflavone; CAR, constitutive androstane receptor; CID, collision-induced dissociation; C_{max}, maximum concentration; DEX, dexamethasone; DMSO, dimethyl sulfoxide; PB, phenobarbital; P450, Cytochrome P450; PXR, pregnane X receptor;

RIF, rifampicin; RLM, rat liver microsomes; TCDD, 2,3,7,8-tetrachloro-dibenzo-dioxin; UGT, UDP-glucuronosyltransferase

ABSTRACT

JNJ-2482272, under investigation as an anti-inflammatory agent, was orally administered to rats *q.d.* at 60 mg/kg for six consecutive days. Despite high plasma exposure after single administration (C_{max} of 7.1 μM), JNJ-2482272 had plasma concentration beneath the lower limit of quantification (3 ng/mL) after six consecutive days of dosing. To determine if JNJ-2482272 is an autoinducer in rats, plated rat hepatocytes were treated with JNJ-2482272 for two days. The major hydroxylated metabolites of JNJ-2482272 were isolated and characterized by MS and NMR analyses. Compared to the vehicle treated cells, a concentration-dependent increase was observed in the formation of Phase I and II-mediated metabolites coinciding with greater expression of P450s and UGTs in rat hepatocytes. CYP1A1, CYP1A2, CYP1B1, and UGT1A6 transcripts were predominantly induced, suggesting that JNJ-2482272 is an activator of the aryl hydrocarbon receptor (AhR). In a human AhR reporter assay, JNJ-2482272 demonstrated potent AhR activation with an EC_{50} value of 0.768 nM, a potency more comparable to the strong AhR activator and toxin 2,3,7,8-tetrachloro-dibenzodioxin (TCDD) than to weaker AhR activators 3-methylcholanthrene (3-MC), β-naphthoflavone (βNF), and omeprazole (OME). In plated human hepatocytes, JNJ-2482272 induced CYP1A1 gene expression with an EC_{50} of 20.4 nM and increased CYP1A activity > 50-fold from basal levels. In human recombinant P450s (rCYPs), JNJ-2482272 was exclusively metabolized by the CYP1 family of enzymes and most rapidly by CYP1A1. The summation of these in vitro findings bridges the in vivo conclusion that JNJ-2482272 is a strong autoinducer in rats and potentially in humans through potent AhR activation.

SIGNIFICANCE STATEMENT

Drugs that induce their own metabolism (autoinducers) can pose challenges in drug development due to their lack of sustained exposures for pharmacology and safety assessment often precluding their development. JNJ-2482272 is demonstrated herein as a strong AhR activator and CYP1A autoinducer, explaining its near complete loss of exposure after repeat administration in rat, that is likely translatable to human (if progressed further) considering its nanomolar potency comparable to “classical” AhR ligands like TCDD despite bearing a “non-classical” drug structure.

INTRODUCTION

The liver harbors a myriad of nuclear receptors capable of activation by xenobiotics to induce the transcriptional and functional expression of drug metabolizing enzymes and transporters (Amacher, 2010). The nuclear receptors most commonly involved as "xenosensors" include the aryl hydrocarbon receptor (AhR), the constitutive androstane receptor (CAR), and the pregnane X receptor (PXR) (Pascussi et al., 2008). AhR activation results in the transcriptional expression of CYP1A1, CYP1A2, CYP1B1 and UGT1A6 (among others) (Denison and Nagy, 2003; Ramadoss et al., 2005; Whitlock, 1999), while CAR and PXR activation induce expression of a number of shared gene subfamilies, notably CYP2B, CYP2C, CYP3A, and UGT1 (di Masi et al., 2009). Prototypical drugs that activate human AhR, PXR, and CAR are omeprazole (OME) (Diaz et al., 1990), rifampicin (RIF) (Lehmann et al., 1998), and phenobarbital (PB) (Kliewer et al., 1998), respectively, with the caveat that PB is also a PXR activator (Sueyoshi et al., 1999).

In clinical settings, drug inducers can cause significant drug-drug interactions due to (1) enhanced clearance of co-administered drugs, (2) increased conversion of pro-drugs to active metabolite(s), and (3) elevated formation of reactive metabolites (Hewitt et al., 2007). Induction of CYP3A by RIF, for example, reduces efficacy of a broad range of drug classes, including beta-adrenergic blockers (Herman et al., 1983), oral contraceptives (LeBel et al., 1998), immunosuppressants (Hebert et al., 1992), and antiretrovirals (Cohen and Meintjes, 2010). PB-mediated P450 induction contributes to the increased conversion of the anti-neoplastic cyclophosphamide into active metabolites (Maezawa et al., 1981). CYP1A1 and CYP1A2 are considered important isoforms involved in the bioactivation of pro-carcinogens (Guengerich et al., 1990; Rendic and Di Carlo, 1997), and their induction through AhR has often been

speculated to be a risk factor for carcinogenesis and other toxicities (Fuhr, 2000; Ma and Lu, 2007).

Autoinducers, drugs that induce enzymes involved in their own metabolism, present additional challenges in the process of drug development. Due to augmented clearance following multiple administrations, plasma exposure of autoinducers can significantly decrease over time which may cause a loss of pharmacological effect and insufficient safety multiples in pre-clinical toxicology species. Autoinduction can halt drugs from further clinical development, as was the case for the potent CYP3A autoinducer MKC-963 under investigation as a platelet aggregation inhibitor (Shimizu et al., 2006). Therefore, timely identification of inducers and autoinducers in drug discovery is critical to avoid late-stage attrition.

JNJ-2482272 [4-(4-methyl-2-(4-(trifluoromethyl)phenyl)thiazole-5-yl)pyrimidine-2-amine] (Fig. 1), an investigational anti-inflammatory agent, demonstrated a dramatic reduction in its plasma exposure in rats after oral *q.d.* administration at 60 mg/kg/day for six consecutive days and was hypothesized to be an autoinducer. To test this hypothesis, in vitro experiments were conducted to (1) assess JNJ-2482272 autoinduction in rat hepatocytes, (2) identify the nuclear receptor responsible for autoinduction, (3) compare potency of JNJ-2482272 to known P450 inducers, and (4) assess its autoinduction potential in human.

MATERIALS AND METHODS

Chemicals and Reagents. The synthetic preparation of JNJ-2482272 is described in its patent application under the designation of Compound 9 (Love, 2003). The following chemicals were obtained through Sigma-Aldrich: 1-amino-benzotriazole (ABT), β-glucuronidase (Catalog # G0501-100KU), β-naphthoflavone (βNF), formic acid-d_2, 3-methylcholanthrene (3-MC), nefazodone, OME, phenacetin, PB, phenytoin, RIF, TCDD, and tolbutamide. Provided as a toluene solution from vendor, TCDD was dried under a stream of nitrogen gas and reconstituted in dimethyl sulfoxide (DMSO) as a 100 μM stock. LC-MS grade water was obtained through J.T. Baker (Phillipsburg, NJ), and LC grade acetonitrile was obtained through EMD Chemicals (Gibbstown, NJ). Deuterated LC solvents were acquired from Cambridge Isotope Laboratories, Inc (Cambridge, MA). Culture reagents for the luciferase reporter cell lines DPX-2 and DRE and for rat and human hepatocytes were purchased through Puracyp, Inc (Carlsbad, CA) and Celsis/IVT (Baltimore, MD), respectively.

Rat Pharmacokinetic Study. All experiments were performed in accordance with the Institute for Laboratory Animal Research Guide for the Care and Use of Laboratory Animals, as well as with internal company policies and guidelines. JNJ-2482272 was formulated in 20% 2-hydroxylpropyl-β-cyclodextrin and administrated by oral gavage *q.d.* to three male Sprague-Dawley rats (Charles River Laboratories, Hollister, California) at 60 mg/kg/day for six consecutive days. Blood (~ 0.25 mL / timepoint) was obtained from the tail vein and transferred to EDTA-coated vials on Day 1 at 1, 2, 4, 8, and 24 h and on Day 6 at 1 and 2 h post-dose, where the same cohort of rats was used for both Day 1 and Day 6 blood collections. Plasma was separated by centrifugation and stored at – 20°C. On the day of bioanalysis, where Day 1 and

Day 6 plasma samples were prepared and analyzed on the same day, 50 µL of plasma was accurately added by pipette and mixed with an equal volume of DMSO. For the 1, 2, and 4 h plasma samples from Day 1, a 10-fold dilution was first made (25 µL of sample was mixed with 225 µL of blank rat plasma) before excising 50 µL and mixing with DSMO. Protein precipitation was facilitated with the addition of 2.5 volumes of acetonitrile containing the internal standard phenytoin followed by mixing for 10 min on a shaker. Upon centrifugation at 5,700 RPM, supernatant was excised and diluted with three volumes of water. Samples were then housed in a 6°C autosampler for the duration of the bioanalysis.

Parent compound concentrations in plasma were quantified by LC-MS/MS using an Agilent 1100 HPLC system interfaced with an API4000 MS/MS System (Applied Biosystems, Concord, Ontario, Canada). Samples were loaded onto a 2.1 x 50 mm 5 µ Ace C4 column (MAC-MOD Analytical, Inc, catalog # ACE-123-0502) run at a flow rate of 0.8 mL/min, using water containing 0.1 % formic acid (A) and acetonitrile containing 0.1 % formic acid (B) as mobile phases. After injection, the initial B composition of 40 % was increased to 95 % B using a linear gradient for 1.5 min, held constant for 1 min at 95 % B, and re-equilibrated for 1 min at 40 % B for an overall run-time of 3.5 min. JNJ-2482272 was quantified by MS/MS in the positive ion mode by monitoring the Q1 > Q3 transition of *m/z* 337.0 to 133.2 with the dwell time, declustering potential, collision energy, and collision cell exit potential set to 150 msec, 106 V, 47 V, and 10 V, respectively. The internal standard phenytoin was quantified by MS/MS in the positive ion mode by monitoring the Q1 > Q3 transition of *m/z* 253.0 to 182.2 with the dwell time, declustering potential, collision energy, and collision cell exit potential set to 120 msec, 51 V, 25 V, and 10 V, respectively. The lower limit of quantification of JNJ-2482272 was 3 ng/mL. All measured concentrations from plasma samples were within the range of the three

quality controls (3, 30, and 300 ng/mL), and the quality controls passed the 4-6-20 rule (Kringle, 1994). The pharmacokinetic parameters (C_{max}, $AUC_{0\text{-}inf}$ and $t_{1/2}$) were calculated using Phoenix WinNonlin Version 6.3 (Certara, Princeton, NJ).

Rat Hepatocyte Induction Study. Freshly plated, pooled (n of 2) male rat hepatocytes were seeded by vendor on 24-well plates with no overlay at a cell density of 350,000 cells/well (Product Number M91651, Celsis/IVT, Baltimore, MD). Cells were cultured by vendor for two days prior to shipment to Janssen R&D. Upon arrival on day 3, the cell medium was replaced with InVitroGRO™ HI media supplemented with *Torpedo* antibiotic mix, and cells were incubated for five hours in a 37°C humidified incubator with 5 % CO_2 atmosphere. Media was aspirated and replaced with antibiotic-supplemented HI media containing JNJ-2482272 at 0.1, 1, and 10 µM or DMSO vehicle for 48 h with fresh compound/vehicle replacement at 24 h. The HI medium contained 0.2% bovine serum albumin. Triplicate wells were used for each assay condition for both the RT-PCR and metabolite identification studies, and all wells had a final DMSO concentration of 0.1 % (*v/v*).

For RT-PCR gene expression, hepatocytes were washed twice in ice-cold PBS (500 µL), lysed in RLT buffer (600 µL) (Qiagen, Gaithersburg, MD), and stored at -80°C. For metabolite identification, hepatocytes after the 48 h incubation period were washed in KHB media twice and freshly incubated with 1 µM JNJ-2482272 at 37°C in KHB media (250 µL) in the presence or absence of the "pan-P450" inhibitor ABT (1 mM). ABT was dissolved in KHB media as a 100 mM stock solution prior to dilution to its working concentration. The final DMSO content was 0.01% (*v/v*). After 1 h, the reaction was terminated by the addition of one volume of ice-

cold 3:1 acetonitrile:methanol spiked with the internal standard nefazodone (6 nM). Cell lysis and protein precipitation was allowed for 20 min on ice followed by mixing samples for 10 min on an orbital shaker. After centrifugation, the supernatants were dried on an EZ-2 Plus™ Evaporator (GeneVac, Ipswich, England) and reconstituted in 250 µL of 1:5 ratio acetonitrile:water for mass spectrometric analysis.

Rat Hepatocyte Cell Viability Study. Freshly plated, pooled (n of 12) male rat hepatocytes were seeded by vendor on a 96-well collagen coated plate with no overlay at a cell density of 50,000 cells/well (Product Number M91653, BioIVT, Baltimore, MD). Cells were cultured by vendor for two days prior to shipment to Janssen R&D. Upon arrival on day 3, the cell medium was replaced with InVitroGRO™ HI media supplemented with *Torpedo* antibiotic mix, and cells were incubated for two hours in a 37°C humidified incubator with 5 % CO_2 atmosphere. Media was aspirated and replaced with antibiotic-supplemented HI media containing JNJ-2482272 at 10, 3.3, 1.1, 0.37, and 0.04 µM; the cytotoxic control doxorubicin at 10 µM; the non-cytotoxic control fexofenadine at 10 µM; or DMSO vehicle for 24 and 48 h with fresh compound/vehicle replacement at 24 h. For 24 h compound treatments, cells were treated with DMSO vehicle for the first 24 h. Triplicate wells were used for each assay condition. The cell viability was determined through a luminescent-based assay measuring cellular ATP following vendor's protocol (ONE-GLO, Promega).

Metabolite Identification. JNJ-2482272 and its metabolites were characterized on an LTQ-Orbitrap XL Mass Spectrometer (ThermoFisher Scientific, Bremen, Germany) interfaced to a

Surveyor autosampler and binary gradient pump (Thermo Finnigan, San Jose, CA). Sample (50 µL) was loaded onto a 4.6 x 150 mm, 3.5 µ Zora SB-C18 column (Agilent, Part Number 863953-902), kept at 40°C. Metabolites were resolved at a flow rate of 0.3 mL/min using water (A) and acetonitrile (B) containing 0.1 % formic acid as mobile phase. Separation was achieved using a 50 min gradient set up as follows: 0 to 5 min, 2 % B; 5 to 37 min linear gradient from 2 to 95 % B; 37 – 43 min, 95 % B. The mass spectrometer was operated in the positive ion mode from 200 – 800 *m/z* at 15,000 resolution using dioctyl phthalate as an internal calibrant. Data-dependent tandem MS spectra were acquired through collision-induced dissociation (CID) at a collision energy of 45 eV and resolution of 7,500 for the three most abundant ions from full scan MS analysis. Additional instrument settings were as follows: 6 V tube lens, 8 V capillary voltage, 3.5 kV electrospray ion voltage, and 300°C capillary temperature.

Metabolites were characterized through mining tandem MS product ion spectra using vendor software (Thermo Xcalibur 2.2) and facilitated using the MS fragmentation prediction software PrISE 2.1.1 developed by Dotmatics Limited (Hill and Mortishire-Smith, 2005). Metabolite levels were compared by dividing the MS peak areas for each metabolite over the internal standard nefazodone and averaged as a biologic triplicate for each assay condition.

β-Glucuronidase Incubation. Samples from the plated rat hepatocyte induction study for metabolism investigations were utilized for additional structural characterization studies using β-glucuronidase. A 200 µL extract from the quenched incubation of 1 µM JNJ-2482272 in rat hepatocytes pre-treated with 10 µM JNJ-2482272 for 48 h was dispensed into 800 µL of 20 mM acetic acid (pH 5) buffer with and without 20,000 Units/mL β-glucuronidase. The reaction was

allowed for 16 h with gentle shaking in a 37°C water bath before being quenched in 1.5 mL ice-cold 3:1 acetonitrile:methanol spiked with the internal standard nefazodone (6 nM). After centrifugation, the supernatants were dried on the EZ-2 Plus™ Evaporator (GeneVac, Ipswich, England) and reconstituted in 250 µL of 1:5 ratio acetonitrile:water for mass spectrometer analysis on the LTQ-Orbitrap XL Mass Spectrometer (as described above).

Preparation and NMR Structural Characterization of M4 and M5. M4 was prepared from a 5 mL reaction of JNJ-2482272 (100 µM, 169 µg) in 2 mg/mL rat liver microsomes (RLM) prepared from rats induced with the CYP1A-inducer βNF (XenoTech, Lenexa, KS). M5 was prepared from a 20 mL reaction of JNJ-2482272 (10 µM, 67 µg) in 2 mg/mL RLM prepared from rats induced with the CYP2B/CYP3A-inducer PB (XenoTech, Lenexa, KS). Incubations were conducted in 100 mM potassium phosphate buffer (pH 7.4), 3 mM $MgCl_2$, and 2 mM NADPH. Incubations were allowed to proceed for 30 min in a 37°C shaking water bath followed by acidification to 0.02 % formic acid and passage through pre-treated Oasis® HLB solid phase extraction cartridges (Part Number WAT094226, Waters, Milford, MA) as 1-2 mL aliquots. Unreacted JNJ-2482272 and its metabolites were eluted using 3 mL of 3:1 acetonitrile:methanol, pooled, and dried using the EZ-2 Plus™ Evaporator (GeneVac, Ipswich, England). Samples were reconstituted in a 50:50 mixture of methanol and DMSO to a concentration of approximately 1 µg/µL based upon starting material JNJ-2482272 amounts.

Separation of metabolites from unreacted JNJ-2482272 was achieved using a Zorbax Bonus-RP column (5 µm, 10 x 250 mm, Agilent Technologies) on an Agilent 1100 HPLC system equipped with a diode array detector. Samples (80 – 100 µL / run) were eluted using a

gradient of 30 – 80% acetonitrile in water containing 0.1% formic acid over 20 minutes. Flow rate was 5 mL/min, and column temperature was set to 30°C. The samples were detected at 240 nm. Fractions of interest were dried on a GenVac centrifugal evaporator and dissolved in $CDCl_3$. NMR spectra were recorded on a Bruker Avance 600 MHz spectrometer using tetramethylsilane-d_{12} (δH 0.00) as the reference. Proton NMR spectra were obtained using Bruker Topspin software, and MestReNova (Mestrelab Research S.L.) was used to process the spectra.

Rat Liver Microsomal Stability Studies. Microsomal stability studies were conducted on a Biomek® FX Robotic Liquid Handling Workstation (Beckman Coulter, Brea, CA), which consisted of a 96-channel pipette head, a 12-postion workstation deck, and a plate incubator. From a 10 mM DMSO stock, JNJ-2482272 was prepared to a working stock concentration of 1 mM in 1:1 acetonitrile:water. JNJ-2482272 (1 μM) was spiked in a reaction mixture consisting of 100 mM potassium phosphate buffer (pH 7.4), 3 mM $MgCl_2$, and 0.5 mg/mL RLM isolated from either male Sprague Dawley rats dosed with corn oil or the CYP1A inducer βNF (XenoTech, Lenexa, KS). The final organic concentration in the incubation was 0.01% DMSO (*v/v*) and 0.045% acetonitrile (*v/v*). The study was conducted in triplicate for each assay condition. The reaction was brought to 37°C and initiated by adding NADPH to a final concentration of 1 mM. After mixing on the plate-deck, 50 μL aliquots were excised from the reaction plate at 0, 5, 10, 20, 40, and 60 min and mixed with four volumes of acetonitrile spiked with 500 μg/nL of the internal standard phenytoin. Samples were then centrifuged at 5,700 rpm for 10 min at 4°C, and supernatant was diluted 1:3 in water.

JNJ-2482272 was quantified on an API4000 MS/MS System (Applied Biosystems, Concord, Ontario, Canada) interfaced with an Agilent 1100 Series HPLC. Samples were loaded onto a 2 x 50 mm, 5 µ Zorbax SB-Phenyl column (Agilent, catalog # 860975-912) under a flow rate of 1.0 mL/min, using water (A) and acetonitrile (B) containing 0.1 % formic acid. After a 25 µL injection, a linear gradient from 5 to 90 % B for 1.5 min was applied and then held at 100 % B for 0.5 min. JNJ-2482272 was quantified by MS/MS in the positive ion mode by monitoring the transition of *m/z* 337.5 to 132.1 with the dwell time, declustering potential, collision energy, and collision cell exit potential set to 100 msec, 100 V, 40 V, and 15 V, respectively. The internal standard phenytoin was quantified by MS/MS in the positive ion mode by monitoring the transition of *m/z* 253.1 to 182.2 with the dwell time, declustering potential, collision energy, and collision cell exit potential set to 80 msec, 96 V, 27 V, and 20 V, respectively. Results from the triplicate study are reported as the average percent JNJ-2482272 remaining relative to the 0 min time-point.

DPX-2 and DRE Reporter Cell Lines. Derived from the human hepatoma cell line HepG2, the DPX-2 and DRE cell lines (Puracyp, Inc, Carlsbad, CA) are stably transfected with a luciferase reporter construct responsive to human PXR and AhR activators, respectively (Trubetskoy et al., 2005; Yueh et al., 2005a; b). Cells were cultured in accordance with vendor protocols. Cells were seeded onto a 96-well luminescent plate at a density of 2.5 x 10^5 cells/well or 3.0 x 10^5 cells/well for DRE and DPX-2 cell lines, respectively. After 16 h, cells were incubated with compounds in Puracyp proprietary dosing media at a final DMSO concentration of 0.1 %. Dosing media contained 10% fetal bovine serum. After 24 h, the luminescence reaction was initiated using the Bright-GLO™ Luciferase Assay System (Promega, Madison, WI) and

measured on the ViewLux UltraHTS Microplate Imager (Perkin Elmer, Turku, Finland). Fold activation values were calculated relative to the response of vehicle-treated cells. The study was conducted in triplicate for each assay condition.

DMSO stock compound solutions were serially diluted in DMSO 1:10 and 1:2 for AhR and PXR studies, respectively. DRE cells were incubated with JNJ-2482272 and known AhR activators at the following concentrations: JNJ-2482272 (10 μM – 1 pM), 3-MC (10 μM – 1 pM), βNF (10 μM – 1 pM), OME (100 μM – 10 pM), and TCDD (0.1 μM – 0.1 pM). DPX-2 cells were incubated with JNJ-2482272 and known PXR activators at the following concentrations: JNJ-2482272 (10 – 0.04 μM), DEX (100 – 0.4 μM), PB (1 – 0.004 mM), and RIF (10 – 0.04 μM).

CAR1 Reporter Cell Line: This study was conducted by Puracyp, Inc (Carlsbad, CA). An expression vector, harboring human CAR1, RXRα, and CYP3A4 enhancers and promoters linked to the luciferase reporter gene, were transfected into the human hepatoma cell line HepG2 (hCAR1). Frozen hCAR1 cells were thawed and seeded onto a clear-bottom 96-well plate at a density of 40,000 cells/well. Plates were maintained at 37°C in an atmosphere of 5% CO_2 and 95% relative humidity overnight to allow for cell recovery. The medium was replaced with media containing JNJ-2482272, the direct CAR activator CITCO, or DMSO vehicle (0.1 %). Test compounds were added to dosing medium from DMSO stocks at the following concentrations for JNJ-2482272 (10, 3.3, 1.1, 0.37, 0.12, and 0.04 μM) and CITCO (20, 10, 5, 1, 0.5, 0.1, and 0.005 μM). Final DMSO content was 0.2% for JNJ-2482272 and 0.1 % for CITCO incubations. The dosing medium contained 10% fetal bovine serum. The study was conducted

in triplicate for each test concentration. Following a measurement of cell viability (as described below), CAR1 activation was subsequently determined on the BioTek Synergy 2 Luminometer following a 5 min incubation at room temperature upon addition of 50 µL ONE-Glo substrate (Promega). The activation data was normalized to cell viability and calculated as the fold response over DMSO vehicle control.

Cell Viability in Reporter Cell Lines: Cell viability studies were conducted by Puracyp, Inc (Carlsbad, CA) in the human reporter cell lines DRE, CAR1, and DPX-2. Cells were seeded at similar densities employed for the aforementioned reporter assays in 96-well plates. JNJ-2482272 was tested at 10 and 1 µM in DRE and DPX-2 cells in duplicate wells and at 10, 3.3, 1.1, 0.37, 0.12, and 0.04 µM in CAR1 cells in triplicate wells. Following 24 h of exposure, the cell viability was determined by replacing the medium with 50 µL of CellTiter-Fluor Reagent (Promega). Cells were incubated for an additional hour before the fluorescence was measured on a BioTek Synergy 2 Luminometer with excitation set at 400 nm and emission at 510 nm.

Human Hepatocyte P450 Induction Study. Cryopreserved human hepatocytes (IVT, Baltimore, MD) either from a single male donor (Lot XGI) or from an equally mixed pool of three individual donors of male and female (Lots SKD, TSD, and IPH) were seeded in a 96-well plate at 0.7 x 10^6 cells/well in InVitroGRO™ HI media supplemented with *Torpedo* antibiotic mix (IVT). Hepatocytes were cultured for 48 h with fresh media replaced every 24 h before JNJ-2482272 and prototypical P450 inducers were added. For the single donor study, seven concentrations of JNJ-24288272 and "classical" AhR activators were prepared from DMSO

stock solutions through 1:10 serial dilutions in DMSO and spiked into HI media to afford the following test concentration ranges: 10 µM – 10 pM for JNJ-2482272, 3-MC, and βNF and 0.1 µM – 0.1 pm for TCDD. Tailored test concentration ranges were prepared through serial dilutions in DMSO and spiked into HI media for the assay reference P450 inducers OME (100, 50, 16.7, 5.6, 1.9, 0.62, and 0.21 µM), PB (3000, 1000, 333.3, 111.1, 37.0, 12.3, and 4.1 µM), and RIF (20, 6.7, 2.2, 0.74, 0.25, 0.082, and 0.027 µM). Doxorubicin and fexofenadine were incubated at 10 µM to serve as cytotoxic and non-cytotoxic reference controls, respectively. For the pooled donor study, test concentrations were as follows: JNJ-2482272 (10, 1, 0.1 and 0.01 µM), βNF (10, 1 and 0.1 µM), OME (10, 1 and 0.1 µM), PB (1 and 0.1 mM), RIF (10 and 1 µM), and TCDD (100, 10, 1, and 0.1 nM). The final DMSO content for all compound incubations was 0.1% *v/v*. HI medium contained 0.2% bovine serum albumin. Basal cell activities were determined from DMSO vehicle (0.1% *v/v*) controls. The study was conducted in triplicate for each assay condition and in duplicate 96-well plates – the first to isolate mRNA for qPCR and the second to measure CYP1A activity and cell viability. Hepatocyte incubation was allowed for 48 h before termination with fresh compound addition at 24 h.

For mRNA analysis by RT-PCR analysis, hepatocytes were washed twice in KHB media (100 µL) and lysed in RLT buffer (Qiagen, Gaithersburg, MD) containing 1% β-mercaptoethanol (100 µL). Lysates were mixed by pipette three times prior to storage at - 80°C for later mRNA extraction.

For CYP1A activity, culture media was subsequently replaced with KHB buffer containing the CYP1A probe substrate phenacetin (50 µM). The reaction (80 µL) was incubated for 30 min in a 37°C cell culture incubator and terminated with the addition of ice-cold 1:1 acetonitrile:methanol (130 µL) spiked with the internal standard phenytoin (0.1 µg/mL). Upon

centrifugation, supernatant was diluted 1:2 in water and subjected to LC-MS/MS analysis on a Schimadzu LC-20AD HPLC System interfaced to an API5000 MS/MS System (Applied Biosystems, Concord, Ontario, Canada). Samples were loaded onto a 2 x 50 mm, 4 µ Synergi Hydro-RP column (Phenomenex, catalog # 00B-4375-B0) heated to 40 °C and placed under a flow rate of 0.5 mL/min, using water (A) and acetonitrile (B) containing 0.1 % formic acid. After a 5 µL injection, a linear gradient from 0 to 95 % B for 2.0 min was applied and held at 95 % B for 0.5 min. The product acetaminophen was quantified by MS/MS in the positive ion mode by monitoring the transition of *m/z* 152.1 > 110.0 with the dwell time, declustering potential, collision energy, and collision cell exit potential set to 80 msec, 52 V, 23 V, and 14 V, respectively. The internal standard phenytoin was quantified by MS/MS in the positive ion mode by monitoring the transition of *m/z* 253.1 > 104.0 with the dwell time, declustering potential, collision energy, and collision cell exit potential set to 80 msec, 36 V, 27 V, and 12 V, respectively. Results from the triplicate study are reported as the average fold change in acetaminophen formation for each compound treatment relative to the vehicle treatment.

For CYP3A activity (pooled donor study only), culture media was subsequently replaced with KHB buffer containing the CYP3A probe substrate midazolam (2 µM). The reaction and sample preparation were conducted similar to the CYP1A conditions described above. Samples were loaded onto a 50 x 2 mm, 4 µ Synergi–Hydro-RP column and eluted at a flow rate of 0.8 mL/min, using water (A) and acetonitrile (B) containing 0.1 % formic acid as mobile phase. Chromatographic separation was achieved using the following conditions: 0% B for 1 min, 0 to 70 % B over 1.5 min followed by 95 % B elution for 1 min. The overall run-time, including re-equilibration, was 4.7 min. The product 1-hydroxy-midazolam was quantified by MS/MS in the positive ion mode by monitoring the transition of *m/z* 342.2 > 297.1 with the dwell time,

declustering potential, collision energy, and collision cell exit potential set to 100 msec, 96 V, 33 V, and 16 V, respectively. Results from the triplicate study are reported as the average fold change in 1-hydroxy-midazolam formation for each compound treatment relative to the vehicle treatment.

Following the CYP1A activity probe reaction for the single donor study, the same plate was used to measure cell viability. Cells were washed twice with KHB buffer (100 µL), and cellular ATP was subsequently measured through a luminescent-based assay following vendor protocol (ONE-GLO, Promega).

RT-PCR Analysis. For rat hepatocyte lysates, total RNA was isolated using the RNeasy Mini kit (Qiagen, Valencia, CA) and prepared for RT-PCR using the High Capacity cDNA Reverse Transcription kit (Applied Biosystems, Foster City, CA). Transcript levels were quantified by RT-PCR on an ABI Prism 7900HT instrument (Applied Biosystems) using TaqMan assays from Applied Biosystem's "Assays on Demand" catalog for studies in rat (CYP1A1, Rn00487218_m1; CYP1A2, Rn00561082_m1; CYP1B1, Rn00564055_m1; CYP2B1, Rn01457875_m1; CYP3A1 / CYP3A23, Rn01640761_gH; and UGT1A6, Rn00756113_mH). Reactions were run in triplicate, and the average threshold cycle (Ct) of GAPDH for each sample was used to normalize Ct values for other transcripts from the same sample.

For human hepatocyte lysates, the RNA isolation and RT-PCR was performed by Infinity Biologix (Piscataway, NJ). In brief, RNA was extracted using the Chemagic RNA Tissue Kit (Art. #1212) and prepared into cDNA with the SuperScript® VILO™ MasterMix first strand synthesis kit. Quantitative RT-PCR was performed using human CYP1A1, CYP1A2, CYP2B6,

or CYP3A4-specific primers/probes (Catalog # Hs01054794_m1, Hs00167927_m1, Hs00167937_g1, or Hs00604506_m1, respectively) using Applied Biosystem's Viia7 Real Time PCR System and analyzed using OmicSoft ArrayStudio V10.0. Ct values for the quantified P450s were normalized to the housekeeping control (18S, Catalog # Hs99999901_s1). For each of the treated samples, the comparative analyses were performed by subtracting the normalized treated values (ΔCt) from the normalized vehicle (control) values to generate ΔΔCt and subsequently fold change, where fold change = $2^{-\Delta\Delta Ct}$.

Recombinant Human P450 Phenotyping. JNJ-2482272 stock solution (10 mM) was prepared in DMSO and diluted to 200 µM in 1:1 acetonitrile:water. The incubation mixture (0.4 mL total volume) consisted of 100 pmol/mL recombinant human P450 (1A1, 1A2, 1B1, 2A6, 2B6, 2C8, 2C9, 2C19, 2D6, or 3A4) or 0.5 mg/mL human liver microsomes, 1 µM JNJ-2482272, and 1 mM NADPH in 100 mM potassium phosphate buffer, pH 7.4. The following supersome and liver microsome lots, all obtained from Corning, were used for this study: 307006 (CYP1A1), 9350005 (CYP1B1), 9095001 (CYP1A2), 0014001 (CYP2A6), 9155002 (CYP2B6), 9193002 (CYP2C8), 0056001 (CYP2C9), 0006001 (CYP2C19), 9274002 (CYP2D6*1), 0002001 (CYP3A4), 9280001 (null vector), and 38294 (human liver microsomes). The protein content in each of the supersome incubations was normalized to 3.4 mg/mL using protein from a null vector supersome control. The final vehicle content in the incubation was 0.01% DMSO (*v/v*) and 0.225% acetonitrile (*v/v*). All incubations were conducted in duplicate. The reaction was initiated with the addition of NADPH; carried out for 0, 15, or 60 min at 37°C; and terminated by addition of 300 µL acetonitrile:methanol (1:1, *v/v*) containing an internal standard (100 nM tolbutamide). Samples were mixed for 1 min and refrigerated. Following the last time point

collection, samples were refrigerated for an additional 20 min prior to centrifugation at 3,100 rpm at 10°C for 20 minutes to precipitate the proteins. The resulting supernatant (20 µL) was then diluted with water (500 µL), and a 5 µL aliquot was injected onto the LC-MS/MS system.

Samples were analyzed by LC-MS/MS in Multiple Reaction Monitoring (MRM) scan mode with positive electrospray ionization (ESI+). The LC-MS/MS system comprised of an API-5500 (Sciex, Redwood City, CA) interfaced with a Shimadzu HPLC system with two LC-30AD pumps, SIL-30ACMP autosampler, column oven, degasser, and a controller (Shimadzu, Columbia, MD). Chromatographic separation for samples was preformed using a Thermo Scientific Hypersil Gold column (3 µm, 50 x 2.1 mm) using a gradient consisted of mobile phases of 0.1 % formic acid in water (A) and 0.1 % formic acid in acetonitrile (B). The gradient was 10 – 60 % B from 0 – 2 min, 60 – 95 % B from 2 – 2.5 min, and 95% B from 2.5 – 3 min at a flow rate of 0.3 mL/min. The Q1 > Q3 MRM transitions for JNJ-2482272 and tolbutamide were 336.9 > 133.1 and 271.1 > 91.0 *m/z*, respectively. Results are reported as the average percent JNJ-2482272 remaining at 15 or 60 min relative to the 0 min time-point.

Conformational Analysis. A conformational analysis was performed to compare JNJ-2482272 to three prototypical “classical” AhR activators (TCDD, βNF, and 3-MC) and three "non-classical" AhR activators (OME, VU0418506, and A-998679). Compound structures were imported into the 2D sketcher in Maestro (Schrödinger ver.2020-2) and then prepared via LigPrep. In LigPrep, the OPLS3e forcefields were used (Roos et al., 2019), retaining the drawn ionization states and the depicted chiralities.

In order to generate 3D conformers of these compounds, the default settings in MacroModel were employed applying the OPLS3e forcefields and using water as the solvent

model. Solvation effects were simulated using the analytical Generalized-Born/Surface-Area (GB/SA) model. For minimization, the Polak-Ribier Conjugate Gradient (PRCG) method was used for a maximum of 5,000 iterations, where convergence was calculated on the gradient at a threshold of 0.05. For the conformational search, the mixed torsional/low-mode sampling mode was applied, eliminating redundant conformers using a maximum atom deviation cutoff of 0.5 Å.

To determine the most probable conformation of JNJ-2482272, a relaxed quantum mechanic dihedral scan was performed along the S-C8-C2-N1 atoms (dashed boxed atoms in Fig. 8) via Jaguar (Bochevarov et al., 2013). A fully analytic scan was performed, rotating the dihedral angle from -180 to 180 in five-degree increments using the 6-31G** basis set and B3LYP theory with no solvent model.

Data Analysis for EC_{50} and E_{max} Determination from Human Reporter and Hepatocyte Transcriptional Studies. Concentration response curves for human reporter (AhR, CAR1, and PXR) and hepatocyte transcriptional studies were fitted in GraphPad Prism 8.0 (GraphPad Software, La Jolla, CA). EC_{50} and E_{max} values were determined from reporter activation concentration-response curves when unambiguous curve fitting was possible. All reported EC_{50} values included the 95% confidence interval. The dose-response curves were fitted to a log (agonist) vs. response plot with variable slope and a baseline value for activation constrained to 1, according to eq. 1:

$$E = 1 + (X\text{^}Hillslope)*(E_{max} - 1)/(X\text{^}HillSlope + EC_{50}\text{^}HillSlope)$$

RESULTS

Repeat Dose Administration of JNJ-2482272 to Rats.

JNJ-2482272 was under pre-clinical investigation as a therapeutic for anti-inflammatory diseases mediated through TNF-α and/or IL12 (Love, 2003). It was orally administered to rats *q.d.* at 60 mg/kg for six consecutive days. On Day 1, JNJ-2482272 exhibited a maximal plasma concentration (C_{max}) of 2,377 $\pm$ 404 ng/mL (~ 7 μM) at 1 h, an area under the curve (AUC) of 5843 $\pm$ 1822 hr*ng/mL, and a $t_{1/2}$ of 1.3 $\pm$ 0.6 h (Fig. 2). After the sixth daily oral dose, JNJ-2482272 concentrations were beneath the level of quantification (< 3 ng/mL) in plasma at 1 and 2 h post-dose, suggesting possible autoinduction.

JNJ-2482272 Induction of P450 and UGT Expression and Cell Viability in Rat Hepatocytes.

Following a 48 h pre-treatment of plated rat hepatocytes with JNJ-2482272 at 0.1, 1, and 10 μM, a 2-fold or greater increase in CYP1A1, CYP1A2, CYP1B1, and UGT1A6 mRNA expression was observed across all concentrations investigated compared to vehicle-treated hepatocytes (0.1 % DMSO) (Table 1). These genes are all members of the AhR gene battery, thereby suggesting that JNJ-2482272 is an AhR activator in rat hepatocytes. JNJ-2482272 also induced the gene expression of CYP2B1 and CYP3A1 / CYP3A23, orthologs to human CYP2B6 and CYP3A4 respectively, but only at the highest tested concentration of 10 μM.

In a separate study, the cell viability was investigated in plated rat hepatocytes for JNJ-2482272 incubated at various concentrations (10 – 0.04 μM) after 24 and 48 h. After 48 h, JNJ-

2482272 caused a mild reduction in viability (~33%) at the 10 μM concentration only (Supplemental Figure 1).

Metabolite Identification in Rat Hepatocytes.

Metabolites were identified after a 1 h incubation of JNJ-2482272 (1 μM) with rat hepatocytes pre-treated for 48 h with vehicle (DMSO 0.1 %) or JNJ-2482272 at 0.1, 1, and 10 μM. The CID spectrum of JNJ-2482272 displayed the product ions at *m/z* 303.0839, 295.0518, 279.0855, 269.0351, 188.9976, 166.0432, 139.0323, 133.0633, and 122.0710 (Fig. 3) obtained through high resolution mass measurements. Proposed structural assignments are depicted in Figure 3 for product ions insightful for metabolite identification. The product ions at *m/z* 295, 269, and 139 were formed through the cleavage of the amino-pyrimidine ring. The product ion at *m/z* 139 also involved the loss of the trifluoromethyl substituted phenyl ring. Scission of the thiazole ring yielded the product ion at *m/z* 166, which underwent a sequential loss of $HS^{\cdot}$ to derive the product ion at *m/z* 133, the most abundant product ion observed in JNJ-2482272 spectrum (Fig. 3), with possible further fragmentation of methyl carbon to afford *m/z* 122.

Rat hepatocyte metabolism of JNJ-2482272 involved both Phase I and II pathways. M4 and M5 were from additions of 16 Da to JNJ-2482272. The CID spectra of M4 and M5 exhibited common product ions at *m/z* 149, 182, and 311, which were 16 Da higher than JNJ-2482272 signature ions at *m/z* 133, 166, and 295 (Table 2), respectively. These observations limit the sites of oxidations to either the methyl substituent of the thiazole or to the pyrimidine moiety. The product ions at *m/z* 269 and 155 were observed in M4 CID spectrum only, suggesting that M4 hydroxylation occurs at the pyrimidine ring *para* to the amino substituent.

This conclusion was further supported by detection of the product ion at *m/z* 242 in M4 spectrum, proposed to be through the loss of the amino-pyrimidine ring. For M5, the product ion at *m/z* 242 was not observed but rather a product ion at *m/z* 258, an addition of 16 Da, thereby excluding the amino-pyrimidine as the site for M5 hydroxylation. In addition, M5 CID spectrum had multiple product ions attributable to the loss of water (e.g., *m/z* 335, 164, and 137), suggestive of an aliphatic hydroxylation. M5 is thus proposed to be result of hydroxylation to the methyl substituent of the thiazole.

Incubation of JNJ-2482272 in RLMs prepared from rats induced with βNF or PB yielded sufficient quantities of M4 and M5, respectively, for structural confirmation by NMR. NMR results are summarized in Table 3, and spectra are included as Supplemental Figures 2 - 4. M4 hydroxylation was localized to the C-5 position of the pyrimidine evidenced by the absence of the C-5 proton of the pyrimidine and the shift of the pyrimidyl C-4 proton from 8.37 ppm in JNJ-2482272 to 8.15 ppm in M4. M5 hydroxylation was localized to the methyl substituent of the thiazole confirmed by the absence of the methyl signal at 2.79 ppm and appearance in signal at 5.00 ppm that integrates to 2.58 protons, corresponding to the oxidized methylene. These assignments were consistent with the above mass spectral localizations for hydroxylation.

Additional metabolites from rat hepatocyte incubations were the result of sequential metabolism. M1, an addition of 192 Da to JNJ-2482272, was one of the major metabolites observed in rat hepatocytes based off UV and MS signal from cold drug. Tandem MS analyses of M1 revealed the product ions at *m/z* 353, 319, 269, 242, 182, and 149, which were also present in the CID spectrum of M4. Incubation of samples with β-glucuronidase depleted M1 concurrent with a rise in M4, substantiating M1 as a glucuronide of M4 (data not shown).

M2 was an addition of 96 Da to JNJ-2482272, and its CID spectrum included the product ions at *m/z* 353, 182, and 149. The product ion *m/z* 353 was the most abundant ion in MS2 spectrum and the result of the neutral loss of 80 Da corresponding to the sulfur trioxide, suggesting M2 is an aryl sulfate. In addition, MS3 spectrum of *m/z* 353 affords *m/z* 182 and 149 as the primary product ions similar in spectral pattern as the hydroxylation M4. Thus, M2 is proposed to be the sulfate conjugate of M4.

Finally, M3 was an addition of 32 Da to JNJ-2482272, and its CID spectrum yielded the product ions at *m/z* 351, 334, 309, 281, 266, and 180. The product ion at *m/z* 351 was derived through a loss of water from $[M+H]^+$ and underwent sequential loss of ammonia to yield the product ion at *m/z* 334. The product ions at *m/z* 309 and 180 is a modification of O – 2H to JNJ-2482272 signature ions at *m/z* 295 and 166 and are considered the result of a loss of water from the di-oxidation modifications of these product ions. Considering the loss of water observed in the CID spectrum of M5 and the prevalence of M4, M3 was proposed to be the product of sequential oxidation of M4 and M5. Furthermore, in hydrogen-deuterium LC-MS exchange experiments, M3 has two additional exchangeable protons relative to JNJ-2482272, consistent with two carbon oxidations. In summation, a proposed metabolic pathway for JNJ-2482272 in rat hepatocytes is presented in Scheme 1.

Autoinduction of JNJ-2482272 Metabolism in Rat Hepatocytes.

In order to relate induction of P450 and UGT gene expression to metabolism of JNJ-2482272, changes in the formation of M1 – M5 were compared in rat hepatocytes either pre-treated with vehicle (basal metabolism) or with ascending concentrations of JNJ-2482272 for 48

h. Levels of M1 and M4, the major rat metabolites, demonstrated a dose-dependent rise in their formation compared to basal levels (Table 4). Pre-treatment of rat hepatocytes with 0.1 μM JNJ-2482272, for example, resulted in a 6.6 and 8.6-fold increase in M1 and M4 formation, respectively, while a 10 μM pre-treatment enhanced M1 and M4 formation 9.2 and 25.5-fold, respectively. The addition of the "pan-P450" inhibitor ABT reduced formation of M1 and M4, implicating P450s as the major contributor to JNJ-2482272 metabolism. No fold increase in formation could be investigated for M2 and M3 since these metabolites were not detected at basal levels. M5 increased after 10 μM JNJ-2482272 pre-treatment only and was not inhibited by ABT at the test concentration of 1 μM.

Metabolic Stability of JNJ-2482272 in CYP1-Enriched Rat Liver Microsomes.

To further relate CYP1 family induction to JNJ-2482272 metabolism, JNJ-2482272 was incubated in RLM obtained from rats dosed with vehicle or the CYP1A-inducer βNF. The half-life of JNJ-2482272 in RLM from naïve treated animals was 91 min (Fig. 4). In RLM from βNF treated animals, JNJ-2482272 half-life was reduced to < 4 min, indicating a substantially increased rate of metabolism in liver microsomes enriched with CYP1 isoenzymes. From samples taken at the 10-minute timepoint, M4 was the major metabolite formed in RLM βNF treated animals, suggesting a role for the CYP1 family of enzymes in its formation (data not shown).

Activation of Human AhR, CAR1, and PXR by JNJ-2482272 in Reporter Cell Lines.

In the human AhR reporter cell line DRE, JNJ-2482272 activated the AhR across all concentrations tested with a 27-fold and 155-fold greater response over vehicle at 1 pM and 10 μM, respectively (Fig. 5A). JNJ-2482272 had an EC_{50} of 0.768 nM, which was ~ 41-fold less potent than the strong AhR activator TCDD (EC_{50} = 0.0186 nM) and greater than three orders of magnitude more potent than the weak AhR activators βNF (EC_{50} = 1,940 nM) and OME (EC_{50} = 18,200 nM). A partial agonist response was observed for 3-MC, which may have been a consequence of its limited solubility at μM test concentrations.

In the human CAR1 reporter cell line, JNJ-2482272 was compared to the direct CAR1 activator CITCO (Fig. 5B). CITCO activated CAR1 with an EC_{50} of 0.305 μM. JNJ-2482272 increased CAR1 activation by > 2-fold at test concentrations of 0.37 μM and higher, achieving a fold-induction of 10.9 at 10 μM. The E_{max} for JNJ-2482272 could not be determined at a top concentration of 10 μM, and its EC_{50} is reported to be > 10 μM.

In the human PXR reporter cell line DPX-2, JNJ-2482272 was compared to the PXR activators DEX, PB, and RIF (Fig. 5C). RIF and PB had EC_{50} values of 1.35 and 313 μM, respectively. Due to incomplete concentration response curves, EC_{50} values were not determined for DEX and JNJ-2482272. JNJ-2482272 produced mild activation only at 10 μM with a 2.3-fold increase over vehicle control, corresponding to a 22% response relative to RIF at 10 μM.

In a fluorescent assay measuring cell viability, JNJ-2482272 at its highest test concentration of 10 μM maintained cell viability (> 80% viability relative to vehicle control) in all human reporter cell lines (Supplemental Figure S5).

JNJ-2482272 Induction of P450 Transcription and CYP1A Activity in Human Hepatocytes.

After a 48 h incubation in human hepatocytes from a single donor, JNJ-2482272 exhibited concentration dependent increases in CYP1A1 and CYP1A2 mRNA expression, augmenting their transcription > 50-fold from the vehicle control, with EC_{50} values of 20.4 and 9.93 nM, respectively (Fig. 6). Similar to findings in the AhR reporter cell line DRE, JNJ-2482272 was two orders of magnitude less potent than TCDD (CYP1A1 EC_{50} = 0.222 nM) and at least three orders of magnitude more potent than βNF and OME. Each CYP1A inducer afforded a comparable concentration response for both CYP1A1 and CYP1A2, supportive of a common mechanism for their induction. In contrast to CYP1A1 and CYP1A2, JNJ-2482272 had only mild induction of CYP2B6 (~ 2-fold across a concentration range from 0.1 to 10 μM) and no induction of CYP3A4 up to 10 μM.

Increases in CYP1A1 and CYP1A2 transcription were also shown to result in higher CYP1A activity in human hepatocytes using the same donor. Both TCDD and JNJ-2482272 induced CYP1A activity by ~ 50-fold over vehicle control at 10 nM and 100 nM, respectively (Fig. 7). In contrast, the less potent CYP1A inducers 3-MC, βNF, and OME did not achieve comparable fold increases even at higher test concentrations. Of note, all CYP1A inducers outside of βNF exhibited declines in CYP1A activity at their highest test concentration, which was not attributable to cytotoxicity (Supplemental Table S1).

Similar gene and activity responses were also achieved when using a pool of human hepatocytes from three individual donors. Notably, JNJ-2482272 at concentrations as low as 10 nM induced the gene expression of CYP1A1, CYP1A2, and CYP1B1 at comparable magnitudes to the more potent TCDD and multiple folds above the weaker AhR inducers βNF and OME (Supplemental Figure S6). Both JNJ-2482272 and TCDD exhibited a similar pattern for CYP1A activity with increases in activity >50-fold followed by a decline at their highest test

concentration (Supplemental Figure S7). In addition, JNJ-2482272 at 10 μM did not induce by >2-fold CYP2B6 or CYP3A4. Thus, the general conclusions made from the single hepatocyte donor data for JNJ-2482272 were consistent with those from a pool of hepatocyte donors.

Metabolism of JNJ-2482272 in Human Liver Microsomes and Recombinant P450s

To understand the role CYP1A plays in human JNJ-2482272 metabolism, JNJ-2482272 was incubated in human liver microsomes (HLMs) and across a panel of human recombinant P450s (rCYPs). In HLMs, JNJ-2482272 exhibited metabolism only in the presence of NADPH, supportive of P450 metabolic involvement. Across the panel of human rCYPs, only CYP1A1 and CYP1A2 were capable of metabolizing JNJ-2482272 by > 20% with CYP1A1 exhibiting the most rapid turnover, resulting in >99% depletion of JNJ-2482272 after a 15 min incubation (Table 5). M4 was confirmed to be the major metabolite produced from the CYP1A1 incubation (data not shown). Overall, this supports a strong role for CYP1A involvement in JNJ-2482272 metabolism.

Physicochemical and Conformational Assessment of JNJ-2482272 Compared to "Classical" and "Non-Classical" AhR Activators.

The physicochemical properties of JNJ-2482272 were compared to known AhR activators categorized either as "classical" AhR activators (βNF, 3-MC, and TCDD) or as "non-classical" AhR activators developed as medicinal agents (A-998679, VU0418506, and OME) in Table 6. The molecular weight for the test set ranges from 248 – 345 g/mol with no discerning differences between the categories. The "classical" AhR activators bear higher CLogP values than the "non-classical" AhR activators particularly when considering 3-MC and TCDD, which

are two log units higher in CLogP than other AhR activators. In addition, the "classical" AhR activators have lower polar surface areas ($\leq$ 30) than those exhibited for "non-classical" AhR activators. JNJ-2482272 possesses physicochemical properties more in line with the "non-classical" AhR activators with a moderate CLogP (3.76) and a high polar surface area (92.9) relative to the test set.

A computational approach was taken to examine the possible three-dimensional conformations for JNJ-2482272 relative to the AhR activator test set (Figure 8). A limited number of conformers were possible for the "classical" AhR activators (two each for βNF and TCDD and only one for 3-MC) attesting to their rigid structure with most conformers either completely flat or just slightly out of plane. Greater flexibility was observed for the "non-classical" AhR activators where 105 and 17 conformers were possible for OME and VU0418506, respectively, with A-998679 having the least conformers possible with four. The conformers for VU0418506 were all flat, whereas none of the conformers for OME were completely flat attributable to the kink introduced by its sulfoxide group. For JNJ-2482272, 15 conformers were possible with some out of plane or some at or close to planarity.

To better determine the most probable conformation of JNJ-2482272, a quantum-mechanical dihedral scan was performed along the S-C8-C2-N1 atoms (dashed box for JNJ-2482272 in Figure 8) by rotating the dihedral angle from -180° to 180° in five degree increments. The lowest energy state for JNJ-2482272 was at a dihedral angle of 0°. Rotation of the dihedral angle away from the 0° point steadily resulted in an energy climb to above 5 kcal/mol at 90° while moving away from the 90° point gradually lowers the energy to its lowest point at planarity (Supplemental Figure 8). These observations indicated that the lowest energy state (and therefore the most likely state) for JNJ-2482272 is at a conformation at or close to planarity, a

property more commonly associated with the "classical" AhR activators. Interestingly, the hydroxylation at the amino substituted pyrimidine to product M4 (the major product of CYP1A metabolism) cannot adopt a planar confirmation (data not shown).

DISCUSSION

JNJ-2482272 was hypothesized to be an autoinducer after a complete loss of its exposure in rats after six daily oral administrations. In vitro observations herein substantiate this hypothesis. First, in rat hepatocytes, JNJ-2482272 was a potent inducer of CYP1A1, CYP1A2, CYP1B1, and UGT1A6. Second, it enhanced its own metabolism in rat hepatocytes, notably to the hydroxylation metabolite M4 and its sequential *O*-glucuronide M1. Third, it had a substantially shorter half-life (< 4 min) in RLMs from rats treated with βNF than from vehicle-treated animals (91 min). Therefore, JNJ-2482272 fulfills the criteria of an autoinducer: it induces enzymes responsible for its metabolism.

In rats, JNJ-2482272 metabolism was primarily through P450s. The pyrimidine hydroxylation M4 and its sequential *O*-glucuronide M1 were increased after pre-treatment of hepatocytes at low concentrations of JNJ-2482272 alongside gains in CYP1A and CYP1B expression. M4 was the major metabolite in RLMs prepared from βNF induced rats suggesting CYP1 metabolism. The methyl hydroxylation M5 increased only at 10 μM JNJ-2482272 alongside a gene induction of CYP2B1 and CYP3A1/3A23. The formation of M5 was highest in RLMs prepared from PB induced rats. We speculate M5 formation is augmented by these inducible P450s, but M5 was not inhibited by ABT in the absence of CYP2B/3A induction.

Phenotyping studies using recombinant enzymes and selective chemical inhibitors are needed to appreciate its etiology in full.

JNJ-2482272 was a strong AhR activator in rat and human hepatocytes. JNJ-2482272 induced rat CYP1A1, CYP1A2, and CYP1B1 mRNA at sub-micromolar and non-cytotoxic concentrations (100 nM) and human CYP1A1 mRNA with an EC_{50} of 20.4 nM. In addition, JNJ-2482272 at μM concentrations was capable of inducing CYP2B and CYP3A enzymes in rat hepatocytes and activating human CAR1 and PXR in reporter cell lines. In this respect, JNJ-2482272 is similar to the AhR activators OME and flutamide, which are pleiotropic inducers at higher concentrations (Coe et al., 2006; Curi-Pedrosa et al., 1994; Masubuchi and Okazaki, 1997). Nonetheless, the induction of CYP2B and CYP3A at 10 μM is not believed relevant to JNJ-2482272 autoinduction when considering its free drug levels. JNJ-2482272 is highly plasma protein bound at 1 μM (> 99%) with 0.36 and 0.24% free in rat and human plasma, respectively. Despite its high C_{max} of ~ 7 μM in rat after a single oral administration of 60 mg/kg, its circulating free drug concentrations are only 0.025 μM (7 μM * 0.0036) and its hepatic concentrations are unlikely to exceed 1 μM even if rat hepatic concentrations are 10-fold higher than plasma. This supports only a role for AhR activation to cause rodent autoinduction.

With respect to human relevance, JNJ-2482272 has an EC_{50} of 0.768 nM in a human AhR reporter assay and 20.4 nM in plated human hepatocytes for CYP1A1 mRNA. These EC_{50} values are uncorrected for protein binding and may underestimate JNJ-2482272 potency considering its high protein binding and the presence of protein in dosing media used for reporter and human hepatocyte studies. Although its efficacious concentrations remain unknown (due to its termination), JNJ-2482272 is anticipated to be a human auto-inducer given both its nM potency to induce CYP1A1 and its high affinity for CYP1A1 metabolism.

Compared to known AhR activators, the EC_{50} values for JNJ-2482272 are ~ two orders of magnitude less potent than TCDD, the most potent known AhR activator, and at least three orders of magnitude more potent than βNF and OME. This clearly demarcates JNJ-2482272 as one of the most potent AhR activators. The potential of JNJ-2482272 to displace [^{3}H]-TCDD from the AhR (and thereby bind to AhR) was not explored in this work and merits investigation given evidence for ligand-independent pathways for AhR activation in rodent through a putative tyrosine kinase pathway by proton pump inhibitors (Lemaire et al., 2004). In addition, the AhR activation potential for its hydroxylated metabolites M4 and M5 is of interest.

Interestingly, in human hepatocytes, treatment with most CYP1A inducers (all but βNF) resulted in a reduction in CYP1A activity at their highest concentration tested. The decline in CYP1A activity did not correspond with a reduction in CYP1A1 gene expression nor in cell viability. CYP1A inhibition by these inducers at higher test concentrations may serve as one explanation. JNJ-2482272 inhibits CYP1A2 with an IC_{50} of 6.4 μM (Supplemental Table 2). OME is reported to be a CYP1A time dependent inhibitor with an IC_{50} of 20.6 μM (Zvyaga et al., 2012), and 3-MC is reported to be a CYP1A2 inhibitor ranging in IC_{50} potency from 0.150 – 4.79 μM (Shimada and Guengerich, 2006; Westerink et al., 2008). Nonetheless, TCDD is not considered a CYP1A inhibitor at test concentrations >300 nM (Westerink et al., 2008). Feedback inhibition in protein expression after sustained induction may serve as an alternative explanation.

Over the past few decades, the once rigid structural motif of “classical” AhR activators has evolved with the discovery of new chemotypes that activate the AhR. AhR activators have often been associated with halogenated aromatic hydrocarbons, such as TCDD; polychlorinated biphenyls; or polycyclic aromatic hydrocarbons, such as 3-MC and benzo[a]pyrene, that are

hydrophobic, often bulky, and bear (or can adopt) a planar confirmation (Denison and Nagy, 2003; Lewis et al., 2002; Mekenyan et al., 1996). The advent of cell-based screening platforms and transcriptomic analysis have identified a number of novel chemotypes that activate the AhR and/or induce CYP1A1 (Coe et al., 2006; Hu et al., 2007; Nagy et al., 2002; Waring et al., 2002) and do not bear the "classical" AhR binding motif.

This untoward property can be found in medicinal agents, whose structures often diverge from the "classical" AhR activators. Marketed drugs such as OME, nimodipine, leflunomide, flutamide, mexiletine, and atorvastatin have been reported to induce CYP1A1 both in vitro and in vivo (Hu et al., 2007). More recent examples of medicinal agents exhibiting untoward CYP1A1 induction as well as autoinduction include VU0418506 and A-998679 (structures presented in Figure 8), both explored for CNS indications pre-clinically. VU0418506, containing an azaindazole with an amino linker to a halogenated phenyl ring, had a 6-fold reduction in its exposure after four days of dosing in rat (Engers et al., 2016). A-998679, harboring a 1,2,4 oxadiazole core substituted at the 3 and 5 position to a cyano-substituted phenyl and pyridine, respectively, exhibited up to a 95% loss of drug after 5 days of dosing at 30 mg in rat (Liguori et al., 2012).

A structural and physicochemical analysis was taken to compare "classical" AhR activators such as βNF, 3-MC, and TCDD to "non-classical" AhR activators such as OME, VU0418506, and A-998679 to better categorize JNJ-2482272. "Classical" AhR activators have a limited number of conformers orientated at or close to planarity, whereas "non-classical" AhR activators exhibited greater flexibility most pronounced for OME with > 100 conformers. Although OME cannot adopt a planar confirmation, all four of the conformers for VU0418506 were planar, indicating that planarity alone is not a distinguishing feature between "classical"

and “non-classical”. Despite multiple possible conformers, the planar conformer for JNJ-2482272 was the most thermodynamically stable. Greater distinctions between categories were observed when considering physicochemical properties, where “classical” activators bear higher lipophilicity and lower polar surface areas than "non-classical” activators. TCDD has a CLogP ~5 log units higher than A-998679 with one fourth of its polar surface area. In this respect, JNJ-2482272 is more consistent with a “non-classical” AhR activator. Its CLogP is in the range of other “non-classical” activators and ~ one to three log units lower than βNF and TCDD, respectively. In addition, its polar surface area is close to OME while three to five-fold higher than βNF and TCDD, respectively.

However, JNJ-2482272 diverges from the “non-classical” activators when considering its potency. The majority of “non-classical” activators have cell-based AhR reporter EC_{50} values often in the μM range (Denison and Nagy, 2003; Hu et al., 2007). VU0418506 and A-998679 have EC_{50} values of 9.8 and 16 μM, respectively, in AhR activation assays (Engers et al., 2016; Liguori et al., 2012). In contrast, JNJ-2482272 has sub-nM potency in such assays commensurate to “classical” AhR activators despite its structural similarities to the “non-classicals”. In this respect, JNJ-2482272 is unique – it bears a “non-classical” AhR activator structure but a “classical” AhR activator potency.

Although historically AhR activation has been associated with carcinogenicity and teratogenicity (Gonzalez and Fernandez-Salguero, 1998; Shimizu et al., 2000; Vorderstrasse et al., 2001), AhR activators can be safe and may have therapeutic potential as anti-inflammatories and anti-neoplastics if their metabolic stability and tissue activation profile can be tuned (Dolciami et al., 2020; Safe et al., 2018; Wang et al., 2020). Nonetheless, the nM potency of JNJ-2482272 raises the relevant question as to when an AhR activator shifts from functioning as

a therapeutic to a toxicant. Due to its strong potential for autoinduction through the AhR, JNJ-2482272 was discontinued as a therapeutic; however, the potency of this “non-classical” AhR activator continues to stoke interest that a potent drug-like AhR activator is achievable albeit with familiar concerns regarding druggability and safety.

ACKNOWLEDGEMENTS

The authors would like to acknowledge Jeffery Cowden and Anita Everson from Janssen Research and Development (La Jolla) and Chris Love and Jean Van Wauwe from Janssen Research and Development (Beerse) for their contribution to this work. The authors would also like to acknowledge Heng Keang (HK) Lim from Janssen Research and Development (Spring House) for his detailed review and insightful suggestions to this manuscript.

AUTHORSHIP CONTRIBUTIONS

Participated in research design: Coe, Volak, and Koudriakova

Conducted experiments: Coe, Feinstein, Higgins, Leung, Skaptason, Tam, Kinong, McAllister, and Lim

Performed data analysis: Coe, Feinstein, Higgins, Scott, Skaptason, Tam, Volak, Kinong, McAllister, and Lim

Wrote or contributed to the writing of the manuscript: Coe, Feinstein, Skaptason, Tam, Volak, McAllister, Bittner, Lim, Hack, and Koudriakova

REFERENCES

Amacher DE (2010) The effects of cytochrome P450 induction by xenobiotics on endobiotic metabolism in pre-clinical safety studies. *Toxicol Mech Methods* **20**:159-166.

Bochevarov AD, Harder E, Hughes TF, Greenwood JR, Braden DA, Philipp DM, Rinaldo D, Halls MD, Zhang J and Friesner RA (2013) Jaguar: A high-performance quantum chemistry software program with strengths in life and materials sciences. *International Journal of Quantum Chemistry* **113**:2110-2142.

Coe KJ, Nelson SD, Ulrich RG, He Y, Dai X, Cheng O, Caguyong M, Roberts CJ and Slatter JG (2006) Profiling the hepatic effects of flutamide in rats: a microarray comparison with classical aryl hydrocarbon receptor ligands and atypical CYP1A inducers. *Drug Metab Dispos* **34**:1266-1275.

Cohen K and Meintjes G (2010) Management of individuals requiring antiretroviral therapy and TB treatment. *Curr Opin HIV AIDS* **5**:61-69.

Curi-Pedrosa R, Daujat M, Pichard L, Ourlin JC, Clair P, Gervot L, Lesca P, Domergue J, Joyeux H, Fourtanier G and et al. (1994) Omeprazole and lansoprazole are mixed inducers of CYP1A and CYP3A in human hepatocytes in primary culture. *J Pharmacol Exp Ther* **269**:384-392.

Denison MS and Nagy SR (2003) Activation of the aryl hydrocarbon receptor by structurally diverse exogenous and endogenous chemicals. *Annu Rev Pharmacol Toxicol* **43**:309-334.

di Masi A, De Marinis E, Ascenzi P and Marino M (2009) Nuclear receptors CAR and PXR: Molecular, functional, and biomedical aspects. *Mol Aspects Med* **30**:297-343.

Diaz D, Fabre I, Daujat M, Saint Aubert B, Bories P, Michel H and Maurel P (1990) Omeprazole is an aryl hydrocarbon-like inducer of human hepatic cytochrome P450. *Gastroenterology* **99**:737-747.

Dolciami D, Ballarotto M, Gargaro M, Lopez-Cara LC, Fallarino F and Macchiarulo A (2020) Targeting Aryl hydrocarbon receptor for next-generation immunotherapies: Selective modulators (SAhRMs) versus rapidly metabolized ligands (RMAhRLs). *Eur J Med Chem* **185**:111842.

Engers DW, Blobaum AL, Gogliotti RD, Cheung YY, Salovich JM, Garcia-Barrantes PM, Daniels JS, Morrison R, Jones CK, Soars MG, Zhuo X, Hurley J, Macor JE, Bronson JJ, Conn PJ, Lindsley CW, Niswender CM and Hopkins CR (2016) Discovery, Synthesis, and Preclinical Characterization of N-(3-Chloro-4-fluorophenyl)-1H-pyrazolo[4,3-

b]pyridin-3-amine (VU0418506), a Novel Positive Allosteric Modulator of the Metabotropic Glutamate Receptor 4 (mGlu4). *ACS Chem Neurosci* **7**:1192-1200.

Fuhr U (2000) Induction of drug metabolising enzymes: pharmacokinetic and toxicological consequences in humans. *Clin Pharmacokinet* **38**:493-504.

Gonzalez FJ and Fernandez-Salguero P (1998) The aryl hydrocarbon receptor: studies using the AHR-null mice. *Drug Metab Dispos* **26**:1194-1198.

Guengerich FP, Shimada T, Iwasaki M, Butler MA and Kadlubar FF (1990) Activation of carcinogens by human liver cytochromes P-450. *Basic Life Sci* **53**:381-396.

Hebert MF, Roberts JP, Prueksaritanont T and Benet LZ (1992) Bioavailability of cyclosporine with concomitant rifampin administration is markedly less than predicted by hepatic enzyme induction. *Clin Pharmacol Ther* **52**:453-457.

Herman RJ, Nakamura K, Wilkinson GR and Wood AJ (1983) Induction of propranolol metabolism by rifampicin. *Br J Clin Pharmacol* **16**:565-569.

Hewitt NJ, Lecluyse EL and Ferguson SS (2007) Induction of hepatic cytochrome P450 enzymes: methods, mechanisms, recommendations, and in vitro-in vivo correlations. *Xenobiotica* **37**:1196-1224.

Hill AW and Mortishire-Smith RJ (2005) Automated assignment of high-resolution collisionally activated dissociation mass spectra using a systematic bond disconnection approach. *Rapid Commun Mass Spectrom* **19**:3111-3118.

Hu W, Sorrentino C, Denison MS, Kolaja K and Fielden MR (2007) Induction of cyp1a1 is a nonspecific biomarker of aryl hydrocarbon receptor activation: results of large scale screening of pharmaceuticals and toxicants in vivo and in vitro. *Mol Pharmacol* **71**:1475-1486.

Kliewer SA, Moore JT, Wade L, Staudinger JL, Watson MA, Jones SA, McKee DD, Oliver BB, Willson TM, Zetterstrom RH, Perlmann T and Lehmann JM (1998) An orphan nuclear receptor activated by pregnanes defines a novel steroid signaling pathway. *Cell* **92**:73-82.

Kringle RO (1994) An assessment of the 4-6-20 rule for acceptance of analytical runs in bioavailability, bioequivalence, and pharmacokinetic studies. *Pharm Res* **11**:556-560.

LeBel M, Masson E, Guilbert E, Colborn D, Paquet F, Allard S, Vallee F and Narang PK (1998) Effects of rifabutin and rifampicin on the pharmacokinetics of ethinylestradiol and norethindrone. *J Clin Pharmacol* **38**:1042-1050.

Lehmann JM, McKee DD, Watson MA, Willson TM, Moore JT and Kliewer SA (1998) The human orphan nuclear receptor PXR is activated by compounds that regulate CYP3A4 gene expression and cause drug interactions. *J Clin Invest* **102**:1016-1023.

Lemaire G, Delescluse C, Pralavorio M, Ledirac N, Lesca P and Rahmani R (2004) The role of protein tyrosine kinases in CYP1A1 induction by omeprazole and thiabendazole in rat hepatocytes. *Life Sci* **74**:2265-2278.

Lewis DF, Jacobs MN, Dickins M and Lake BG (2002) Quantitative structure--activity relationships for inducers of cytochromes P450 and nuclear receptor ligands involved in P450 regulation within the CYP1, CYP2, CYP3 and CYP4 families. *Toxicology* **176**:51-57.

Liguori MJ, Lee CH, Liu H, Ciurlionis R, Ditewig AC, Doktor S, Andracki ME, Gagne GD, Waring JF, Marsh KC, Gopalakrishnan M, Blomme EA and Yang Y (2012) AhR activation underlies the CYP1A autoinduction by A-998679 in rats. *Frontiers in genetics* **3**:213.

Love CJVW, Jean Pierre Frans; De Brabander, Marc J.; Moses, Roger Clive; Goncharenko, Mykhalyo; Cooymans, Ludwig Paul; Vandermaesen, Nele; Diels, Gaston Stanislas Marcella; Sibley, Anthony William; Noula, Caterina. (2003) 2,4,5-Trisubstituted Thiazolyl Derivatives and Their Antiinflammatory Activity.

Ma Q and Lu AY (2007) CYP1A induction and human risk assessment: an evolving tale of in vitro and in vivo studies. *Drug Metab Dispos* **35**:1009-1016.

Maezawa S, Ohira S, Sakuma M, Matsuoka S, Wakui A and Saito T (1981) Effects of inducer of liver drug-metabolizing enzyme on blood level of active metabolites of cyclophosphamide in rats and in cancer patients. *Tohoku J Exp Med* **134**:45-53.

Masubuchi N and Okazaki O (1997) An evaluation of the CYP1A induction potential of pantoprazole in primary rat hepatocytes: a comparison with other proton pump inhibitors. *Chem Biol Interact* **107**:63-74.

Mekenyan OG, Veith GD, Call DJ and Ankley GT (1996) A QSAR evaluation of Ah receptor binding of halogenated aromatic xenobiotics. *Environ Health Perspect* **104**:1302-1310.

Nagy SR, Liu G, Lam KS and Denison MS (2002) Identification of novel Ah receptor agonists using a high-throughput green fluorescent protein-based recombinant cell bioassay. *Biochemistry* **41**:861-868.

Pascussi JM, Gerbal-Chaloin S, Duret C, Daujat-Chavanieu M, Vilarem MJ and Maurel P (2008) The tangle of nuclear receptors that controls xenobiotic metabolism and transport: crosstalk and consequences. *Annu Rev Pharmacol Toxicol* **48**:1-32.

Ramadoss P, Marcus C and Perdew GH (2005) Role of the aryl hydrocarbon receptor in drug metabolism. *Expert Opin Drug Metab Toxicol* **1**:9-21.

Rendic S and Di Carlo FJ (1997) Human cytochrome P450 enzymes: a status report summarizing their reactions, substrates, inducers, and inhibitors. *Drug Metab Rev* **29**:413-580.

Roos K, Wu C, Damm W, Reboul M, Stevenson JM, Lu C, Dahlgren MK, Mondal S, Chen W, Wang L, Abel R, Friesner RA and Harder ED (2019) OPLS3e: Extending Force Field Coverage for Drug-Like Small Molecules. *J Chem Theory Comput* **15**:1863-1874.

Safe S, Han H, Goldsby J, Mohankumar K and Chapkin RS (2018) Aryl Hydrocarbon Receptor (AhR) Ligands as Selective AhR Modulators: Genomic Studies. *Curr Opin Toxicol* **11-12**:10-20.

Shimada T and Guengerich FP (2006) Inhibition of human cytochrome P450 1A1-, 1A2-, and 1B1-mediated activation of procarcinogens to genotoxic metabolites by polycyclic aromatic hydrocarbons. *Chem Res Toxicol* **19**:288-294.

Shimizu T, Akimoto K, Yoshimura T, Niwa T, Kobayashi K, Tsunoo M and Chiba K (2006) Autoinduction of MKC-963 [(R)-1-(1-cyclohexylethylamino)-4-phenylphthalazine] metabolism in healthy volunteers and its retrospective evaluation using primary human hepatocytes and cDNA-expressed enzymes. *Drug Metab Dispos* **34**:950-954.

Shimizu Y, Nakatsuru Y, Ichinose M, Takahashi Y, Kume H, Mimura J, Fujii-Kuriyama Y and Ishikawa T (2000) Benzo[a]pyrene carcinogenicity is lost in mice lacking the aryl hydrocarbon receptor. *Proc Natl Acad Sci U S A* **97**:779-782.

Sueyoshi T, Kawamoto T, Zelko I, Honkakoski P and Negishi M (1999) The repressed nuclear receptor CAR responds to phenobarbital in activating the human CYP2B6 gene. *J Biol Chem* **274**:6043-6046.

Trubetskoy O, Marks B, Zielinski T, Yueh MF and Raucy J (2005) A simultaneous assessment of CYP3A4 metabolism and induction in the DPX-2 cell line. *AAPS J* **7**:E6-13.

Vorderstrasse BA, Steppan LB, Silverstone AE and Kerkvliet NI (2001) Aryl hydrocarbon receptor-deficient mice generate normal immune responses to model antigens and are resistant to TCDD-induced immune suppression. *Toxicol Appl Pharmacol* **171**:157-164.

Wang XS, Cao F, Zhang Y and Pan HF (2020) Therapeutic potential of aryl hydrocarbon receptor in autoimmunity. *Inflammopharmacology* **28**:63-81.

Waring JF, Gum R, Morfitt D, Jolly RA, Ciurlionis R, Heindel M, Gallenberg L, Buratto B and Ulrich RG (2002) Identifying toxic mechanisms using DNA microarrays: evidence that an experimental inhibitor of cell adhesion molecule expression signals through the aryl hydrocarbon nuclear receptor. *Toxicology* **181-182**:537-550.

Westerink WM, Stevenson JC and Schoonen WG (2008) Pharmacologic profiling of human and rat cytochrome P450 1A1 and 1A2 induction and competition. *Arch Toxicol* **82**:909-921.

Whitlock JP, Jr. (1999) Induction of cytochrome P4501A1. *Annu Rev Pharmacol Toxicol* **39**:103-125.

Yueh MF, Kawahara M and Raucy J (2005a) Cell-based high-throughput bioassays to assess induction and inhibition of CYP1A enzymes. *Toxicol In Vitro* **19**:275-287.

Yueh MF, Kawahara M and Raucy J (2005b) High volume bioassays to assess CYP3A4-mediated drug interactions: induction and inhibition in a single cell line. *Drug Metab Dispos* **33**:38-48.

Zvyaga T, Chang SY, Chen C, Yang Z, Vuppugalla R, Hurley J, Thorndike D, Wagner A, Chimalakonda A and Rodrigues AD (2012) Evaluation of six proton pump inhibitors as inhibitors of various human cytochromes P450: focus on cytochrome P450 2C19. *Drug Metab Dispos* **40**:1698-1711.

FOOTNOTES

Financial Disclosure: No author has an actual or perceived conflict of interest with the contents of this article. This work received no external funding.

LEGEND FOR FIGURES

Figure 1. Structure of JNJ-2482272 [4-(4-methyl-2-(4-(trifluoromethyl)phenyl)thiazole-5-yl)pyrimidine-2-amine].

Figure 2. Rat Plasma Concentration of JNJ-2482272 on Day 1.

Male Sprague-Dawley rats (n = 3) were dosed orally with 60 mg/kg of JNJ-2482272 once daily as a solution for six consecutive days, and compound exposure in plasma was measured after the first and last day of compound dosing. Detectable levels (> 3 ng/mL) of JNJ-2482272 were only observed in plasma samples after Day 1 of dosing. All data is reported as a mean with standard deviations.

Figure 3. The Product Ion Mass Spectrum of JNJ-2482272 and its Proposed Fragmentation.

Scheme 1. Biotransformation of JNJ-2482272 in Rat Hepatocytes.

Figure 4. Rat Microsomal Stability of JNJ-2482272.

JNJ-2482272 (1 μM) was incubated in 0.5 mg/mL liver microsomes isolated from rats dosed with either corn oil (Naïve RLM) or βNF. The percent of JNJ-2482272 remaining over a 1 h time course was determined through LC-MS/MS by comparing the peak area ratios relative to the peak area ratio observed at t = 0 min. All data is reported as a mean with standard deviations.

Figure 5. Human AhR, CAR1, and PXR Reporter Studies.

JNJ-2482272 was compared to known P450 inducers in the human AhR reporter cell line DRE (A), the human CAR1 reporter cell line (B), and the human PXR reporter cell line DPX2 (C). For the AhR and PXR reporter assays, luciferase reporter activity was measured following incubation with compound for 24 h, and the response with compound treatments are reported as the fold response over vehicle controls cells treated with 0.1 % DMSO. For the CAR1 reporter assay, the luciferase activity after 24 h compound treatment was normalized to cell viability and reported as the fold response to 0.1% DMSO-treated cells. All data is reported as a mean with standard deviations.

Figure 6. Induction of P450 Gene Expression in Human Hepatocytes.

Plated human hepatocytes were treated with JNJ-2482272 and known P450 inducers for 48 h followed by isolation of mRNA for RT-PCR. Fold induction of CYP1A1, CYP1A2, CYP2B6, and CYP3A4 (A – D) is relative to levels expressed in hepatocytes treated with the vehicle control 0.1 % DMSO. All data is reported as a mean with standard deviations.

Figure 7. Induction of CYP1A Activity in Human Hepatocytes.

Plated human hepatocytes were treated with JNJ-2482272 and known P450 inducers for 48 h followed by a 30 min reaction using the CYP1A probe substrate phenacetin. Acetaminophen, the metabolite of phenacetin, was quantified by LC-MS/MS to determine the CYP1A activity. Fold induction is relative to activity in hepatocytes treated with the vehicle control 0.1 % DMSO. All data is reported as a mean with standard deviations.

Figure 8. Conformational Assessment of JNJ-2482272 to Known AhR Activators.

The structures and the three-dimensional conformers are presented for JNJ-2482272 relative to known AhR activators categorized either as “Classical” AhR Activators (βNF, 3-MC, and TCDD) or as “Non-Classical” AhR Activators (A-998679, OME, and VU0418506). The conformers for each AhR activator were superposed as follows: JNJ-2482272, on the 4-methyl-2-(4-(trifluoromethyl)phenyl)thiazole) core; βNF, on the 4H-pyran-4-one core; TCDD, on the dioxin core; A998679, on the oxadiazole core; OME, on the 2-hydrosulfinyl-6-methoxy-1H-benzo[d]imidazole core; and VU0418506, on the azaindazole ring system.

TABLES

Table 1: JNJ-2482272 Fold Induction of P450s and UGT1A6 mRNA in Rat Hepatocytes. Plated rat hepatocytes were treated with JNJ-2482272 or vehicle (0.1 % DMSO) in triplicate for 48 h followed by lysis and RNA isolation for RT-PCR analyses. Fold induction is relative to vehicle control expression levels.

	Fold Induction over Vehicle Control					
JNJ-2482272 (µM)	**CYP1A1**	**CYP1A2**	**CYP1B1**	**CYP2B1**	**CYP3A1 / CYP3A23**	**UGT1A6**
0.1	7.7 ± 0.5	6.8 ± 1.3	181.7 ± 16.4	1.5 ± 0.7	1.6 ± 0.3	2.4 ± 0.1
1	8.5 ± 1.1	6.0 ± 1.4	570.2 ± 60.9	0.9 ± 0.1	1.1 ± 0.2	2.2 ± 0.2
10	16.1 ± 1.6	16.9 ± 6.0	1438.1 ± 290.9	7.8 ± 4.7	9.3 ± 5.9	3.2 ± 0.4

Table 2: Product Ions Formed by Collision-Induced Dissociation (CID) of JNJ-2482272 and its Metabolites.

Analyte	$[M+H]^+$ (*m/z*)	RT (min)	$LC\text{-}MS^n$ Product Ions (*m/z*)
JNJ-2482272	337.0727	37.5	122, 133, 139, 166, 189, 269, 279, 295, 303
M1	529.0995	27.5	149, 182, 242, 269, 319, 353
M2	433.0244	29.6	149, 182, 353
M3	369.0625	30.1	180, 266, 281, 309, 334, 351
M4	353.0675	32.7	149, 155, 182, 242, 269, 311, 319, 325
M5	353.0676	33.0	137, 149, 164, 182, 189, 258, 308, 311, 335

RT, retention time

DMD Fast Forward. Published on June 9, 2022 as DOI: 10.1124/dmd.121.000825
This article has not been copyedited and formatted. The final version may differ from this version.

Table 3: Chemical Shifts for JNJ-2482272 and its Metabolites M4 and M5. M4 and M5 were biochemically synthesized from incubations of JNJ-2482272 in RLM enriched with CYP1A or CYP2B/CYP3A isoforms. Spectra of HPLC-purified metabolites were compared to the spectrum of JNJ-2482272

	JNJ2482272			**M4**			**M5**		
	Shift	*Integration*	*Splitting*	*Shift*	*Integration*	*Splitting*	*Shift*	*Integration*	*Splitting*
A	8.37	0.84	Doublet	8.15	1.08	Singlet	8.38	0.95	Doublet
B	8.09	2.00	Doublet	8.10	2.00	Doublet	8.10	2.00	Doublet
C	7.71	2.09	Doublet	7.71	2.22	Doublet	7.73	2.10	Doublet
D	6.94	1.15	Doublet				6.87	1.06	Doublet
E	2.79	2.92	Singlet	2.71	2.89	Singlet	5.00	2.58	Singlet

Table 4: Fold Change in JNJ-2482272 Metabolite Formation in Rat Hepatocytes Pre-treated with JNJ-2482272. Following a 48 h pre-incubation in the vehicle control (0.1 % DMSO) or JNJ-2482272 (0.1, 1, and 10 μM), plated rat hepatocytes were incubated with JNJ-2482272 (1 μM) for 1 h. All conditions were performed in triplicate, including a co-incubation of JNJ-2482272 (1 μM) with the P450 inhibitor ABT (1 mM). JNJ-2482272 metabolites were compared using mass spectral counts of metabolites normalized to the internal standard nefazodone, where the fold change in metabolite level is relative to vehicle control levels. Metabolites detected only in rat hepatocytes induced with JNJ-2482272 are denoted by a plus (+). n/d = not detected.

		Fold Change in Metabolite Levels over Vehicle Pre-treatment			
	Biotransformation	**0.1 μM**	**1 μM**	**10 μM**	**1 μM + ABT**
M1	***Hydroxylation + Glucuronidation***	**6.6 ± 0.2**	**7.2 ± 0.2**	**9.2 ± 0.7**	**1.2 ± 0.1**
M2	***Hydroxylation + Sulfation***	+	+	+	**n/d**
M3	***Dihydroxylation***	**n/d**	**n/d**	+	**n/d**
M4	***Hydroxylation***	**8.6 ± 0.9**	**10.2 ± 0.5**	**25.5 ± 1.5**	**1.2 ± 0.2**
M5	***Hydroxylation***	**0.1 ± 0.1**	**0.2 ± 0.1**	**13.0 ± 3.2**	**0.2 ± 0.0**

DMD Fast Forward. Published on June 9, 2022 as DOI: 10.1124/dmd.121.000825
This article has not been copyedited and formatted. The final version may differ from this version.

Table 5: Recombinant Human P450 Phenotyping. JNJ-2482272 (1 μM) was incubated in either human liver microsomes (HLM) in the presence (+) and absence (-) of the co-factor NADPH or in various recombinant human P450 isoforms with NADPH for 15 and 60 min. The percent of JNJ-2482272 remaining over the time course (relative to compound levels observed at t = 0 min) was determined through LC-MS/MS.

	Percent of JNJ-2482272 Remaining											
Time (min)	**HLM + NADPH**	**HLM - NADPH**	**1A1**	**1A2**	**1B1**	**2A6**	**2B6**	**2C8**	**2C9**	**2C19**	**2D6**	**3A4**
15	100	109	0.58	28.5	88.7	100	96.3	103	104	97.5	99.6	96.1
60	88.0	103	0.0	12.6	87.4	97.0	92.9	102	103	97.3	101	98.3

Table 6: Physicochemical Properties of JNJ-2482272 and Known AhR Activators.

AhR Activator	Molecular Weight (g/mol)	CLogP	Polar Surface Area (Å)
JNJ-2482272	336	3.76	92.9
TCDD	322	6.45	18.5
βNF	272	4.65	30.2
3-MC	268	6.62	0
OME	345	2.57	96.3
VU0418506	263	4.34	53.6
A-998679	248	1.72	75.6

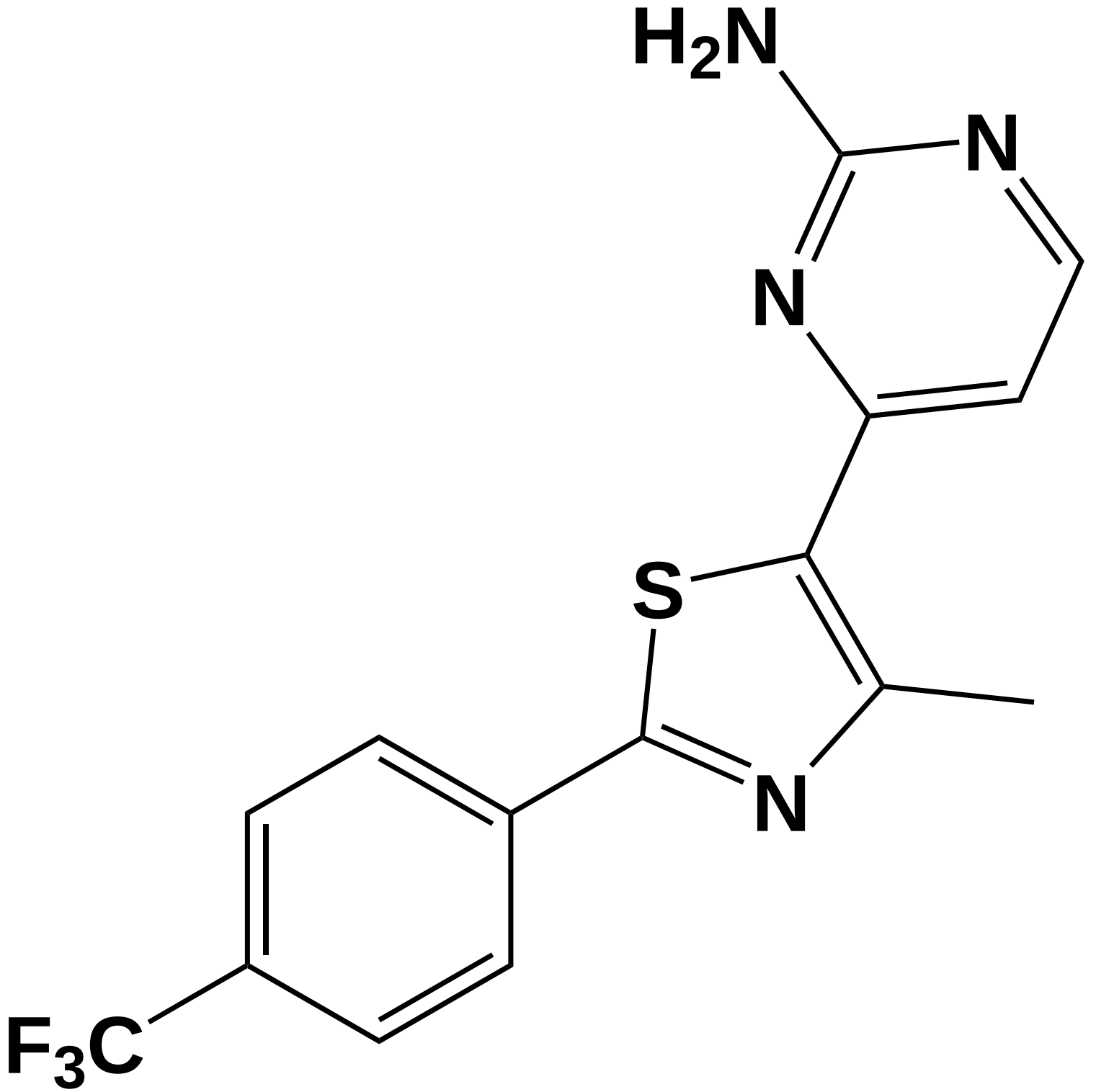

Figure 1

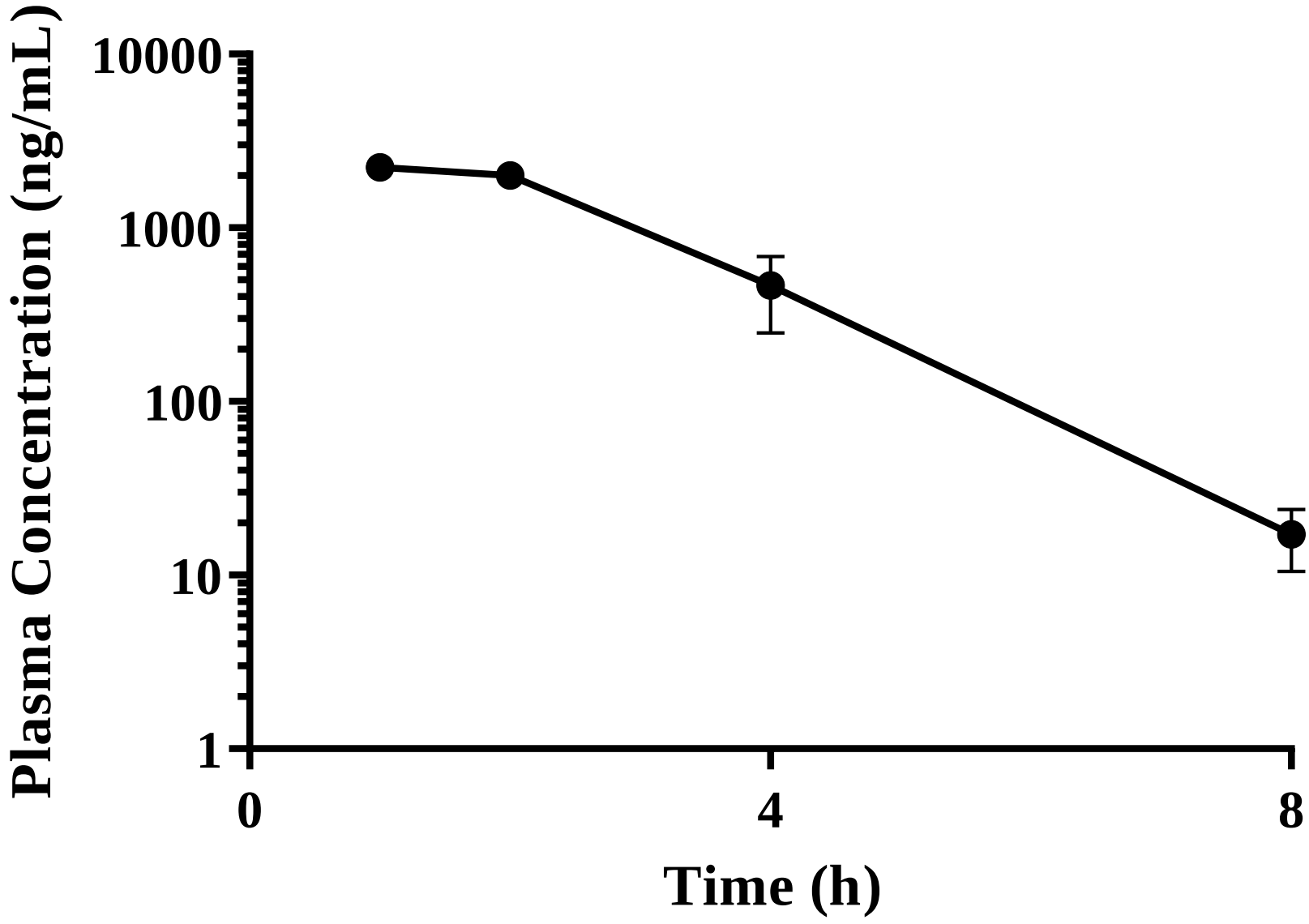

Figure 2

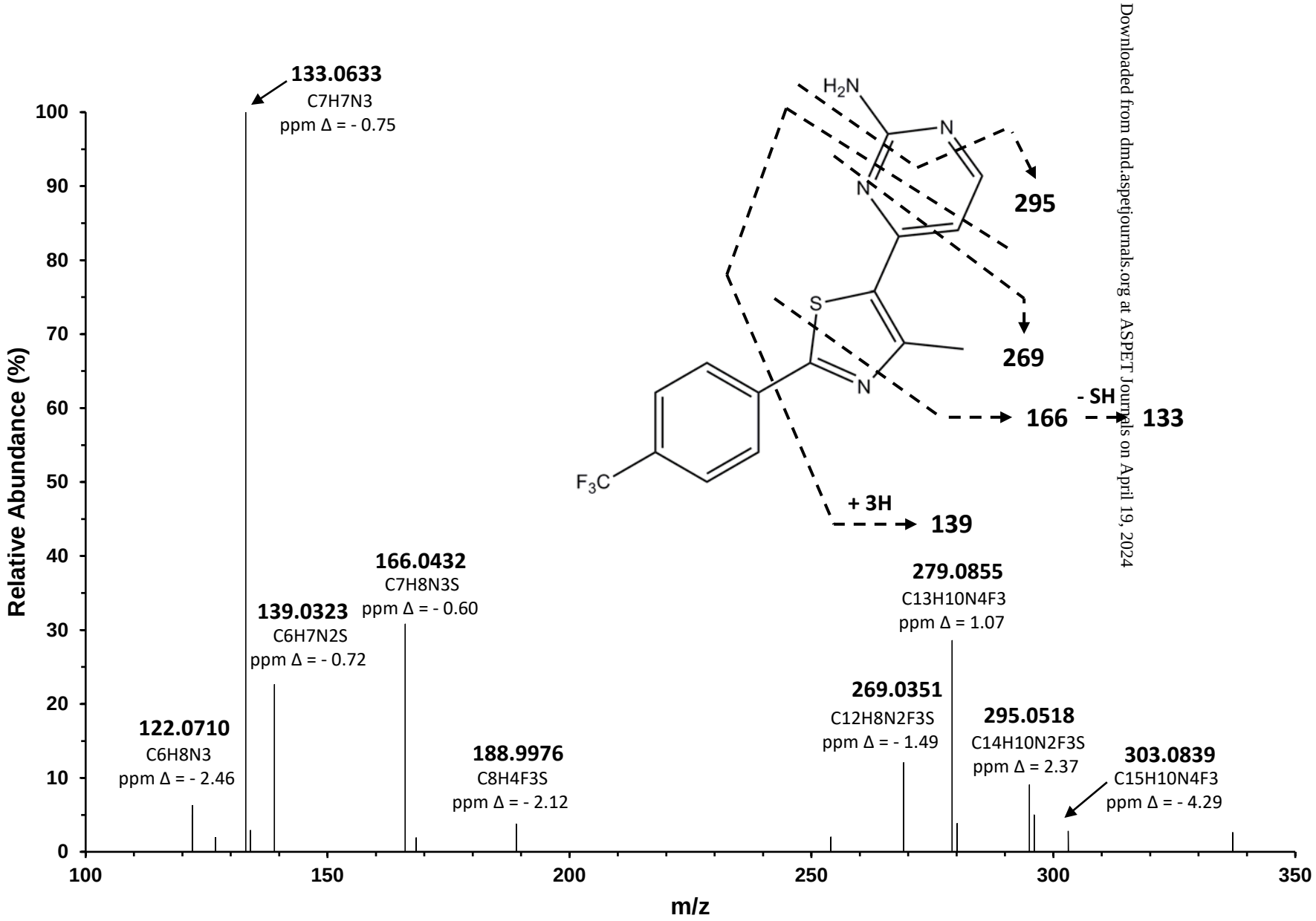

Figure 3

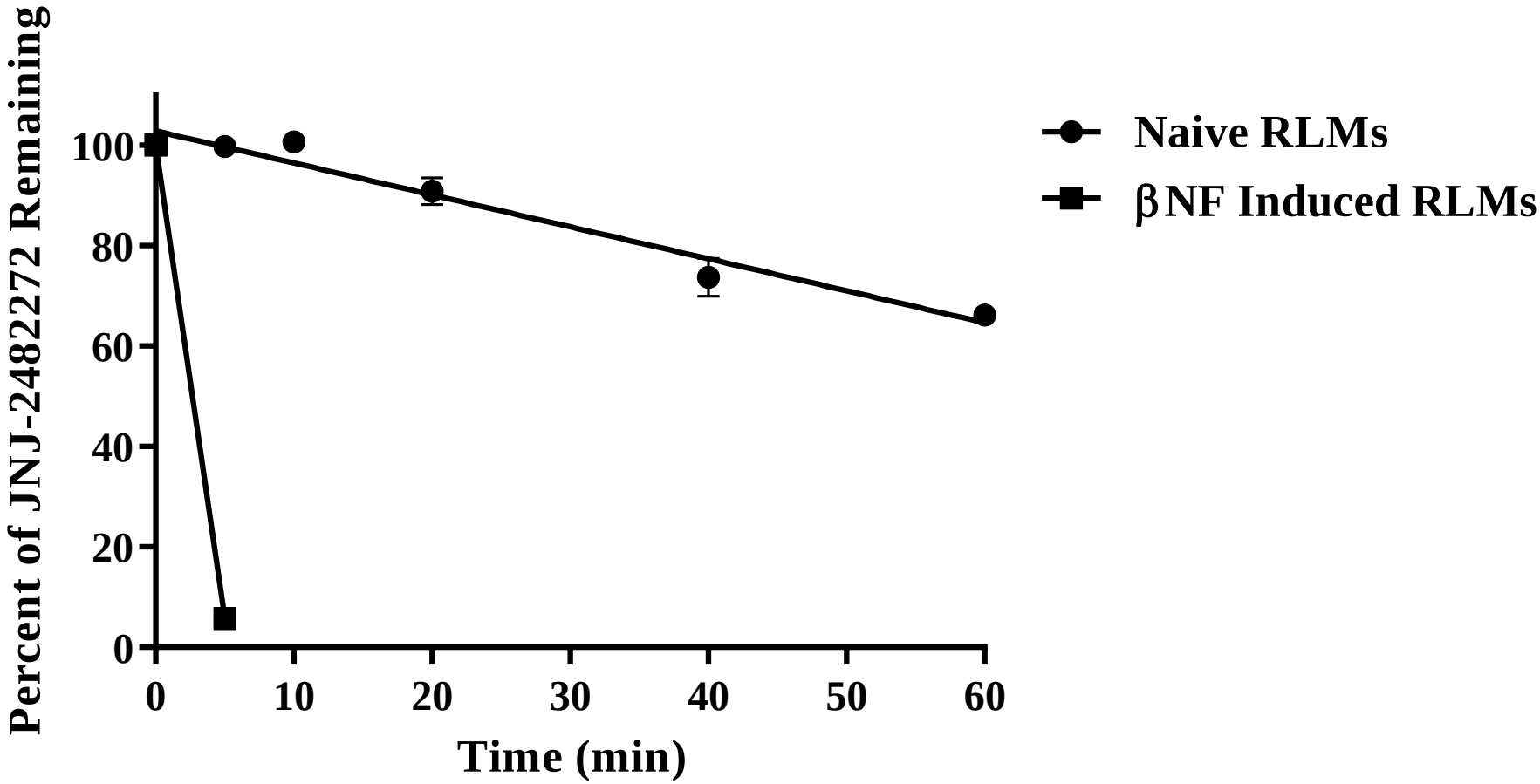
Percent of JNJ-2482272 Remaining
100
80
60
40
20
0
0
10
20
30
40
50
60
Time (min)
Naive RLMs
βNF Induced RLMs

Figure 4

(A)

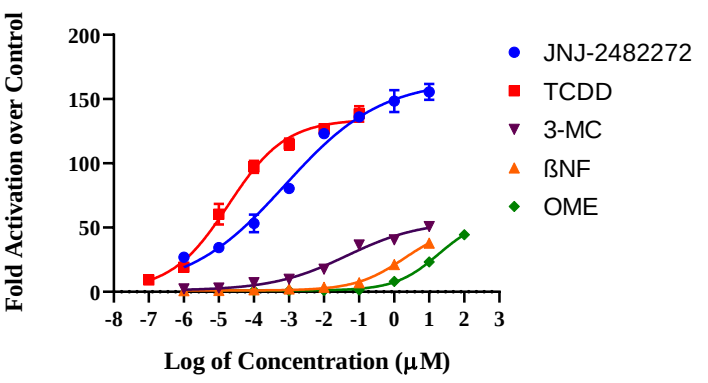

Compound	E_{max}	EC_{50} (nM)	95% Confidence Interval (nM)
JNJ-2482272	165	0.768	0.430 - 1.57
TCDD	134	0.0186	0.0126 - 0.0287
3-MC	55.1	44.2	21.5 - 133
βNF	51.2	1940	1260 - 3860
OME	57.5	18200	13700 - 27200

(B)

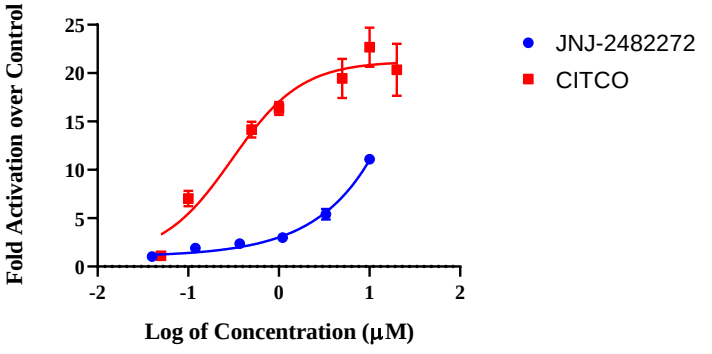

Compound	E_{max}	EC_{50} (nM)	95% Confidence Interval (nM)
JNJ-2482272	ND	> 10000	ND
CITCO	21.2	305	0.0126 - 0.0287

(C)

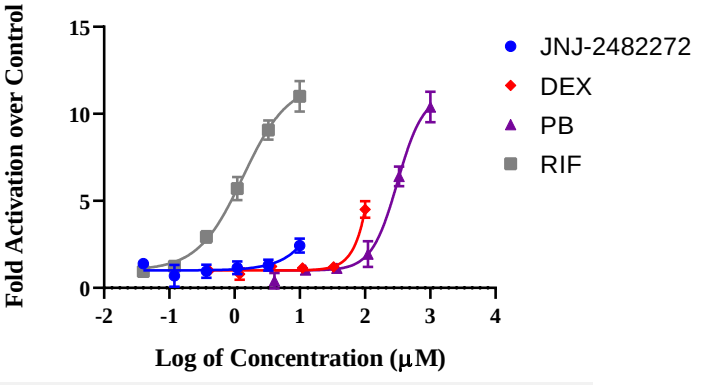

Compound	E_{max}	EC_{50} (µM)	95% Confidence Interval (µM)
JNJ-2482272	ND	> 10000	ND
DEX	ND	> 10000	ND
PB	11.1	313	264 - 435
RIF	11.8	1.35	1.05 - 1.90

Figure 5

(A)

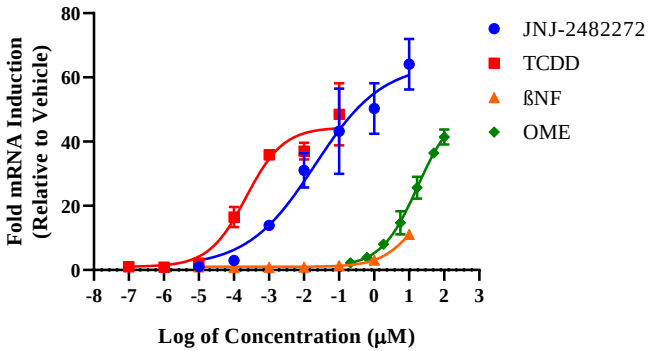

Compound	E_{max}	EC_{50} (nM)	95% Confidence Interval (nM)
JNJ-2482272	64.4	20.4	5.29 - 344
TCDD	44.4	0.222	0.110 - 0.633
OME	50.9	17400	11000 - 39200
βNF	ND	>10000	ND

(B)

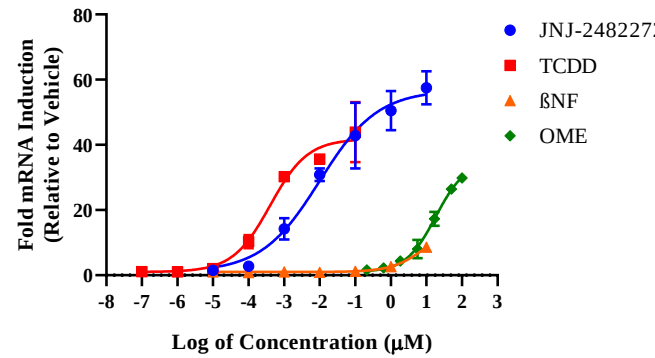

Compound	E_{max}	EC_{50} (nM)	95% Confidence Interval (nM)
JNJ-2482272	56.8	9.93	4.38 - 30.4
TCDD	41.8	0.404	0.220 - 0.934
OME	34.9	18100	13100 - 30900
βNF	ND	>10000	ND

(C)

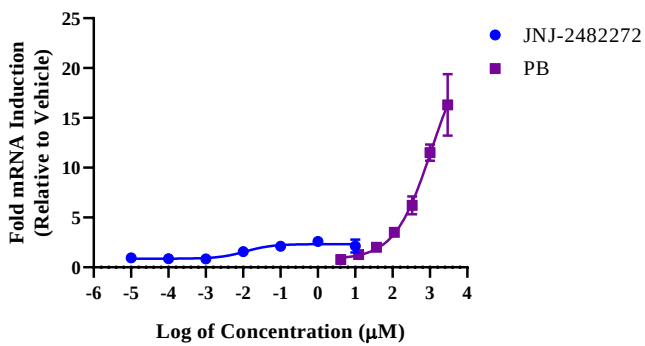

Compound	E_{max}	EC_{50} (mM)	95% Confidence Interval (mM)
PB	22.8	1.10	ND

(D)

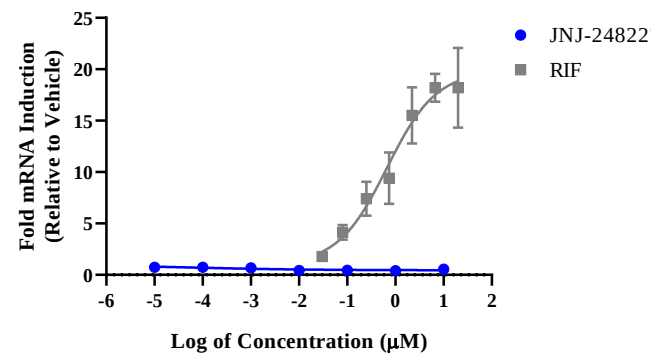

Compound	E_{max}	EC_{50} (nM)	95% Confidence Interval (nM)
RIF	19.8	670	360 - 1950

Figure 6

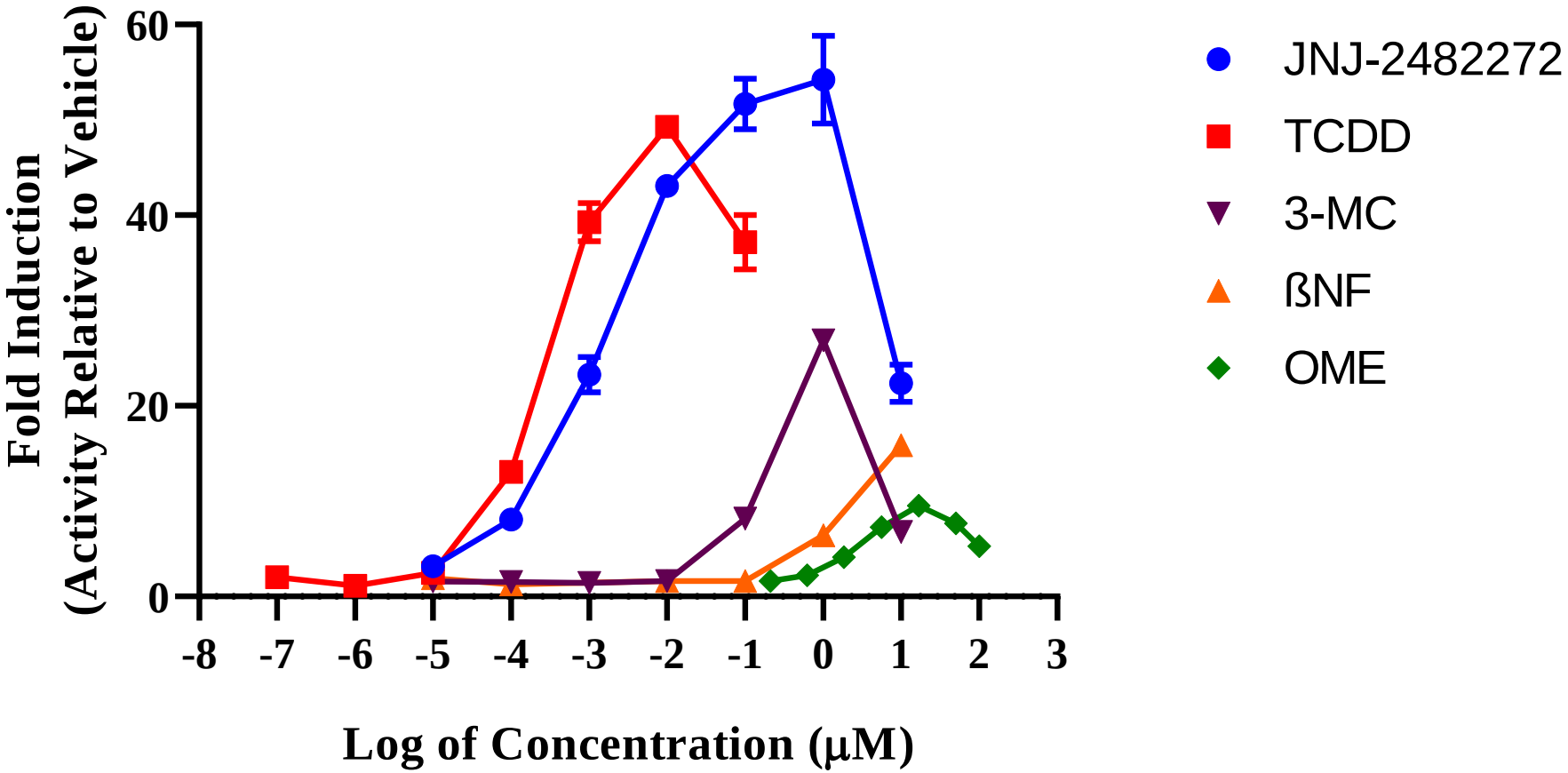
Fold Induction
(Activity Relative to Vehicle)
60
40
20
0
-8
-7
-6
-5
-4
-3
-2
-1
0
1
2
3
Log of Concentration (µM)
JNJ-2482272
TCDD
3-MC
ßNF
OME

Figure 7

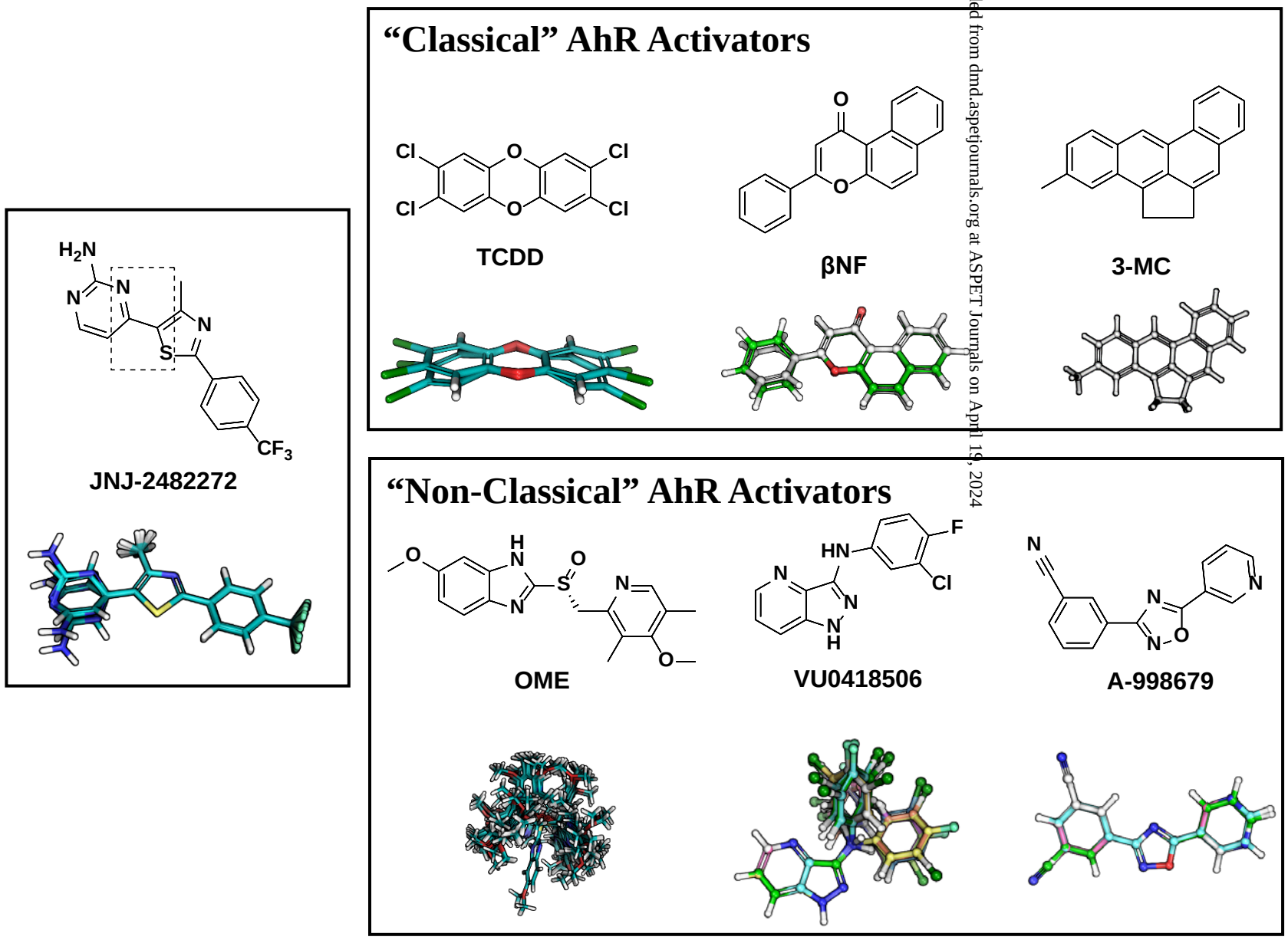

Figure 8

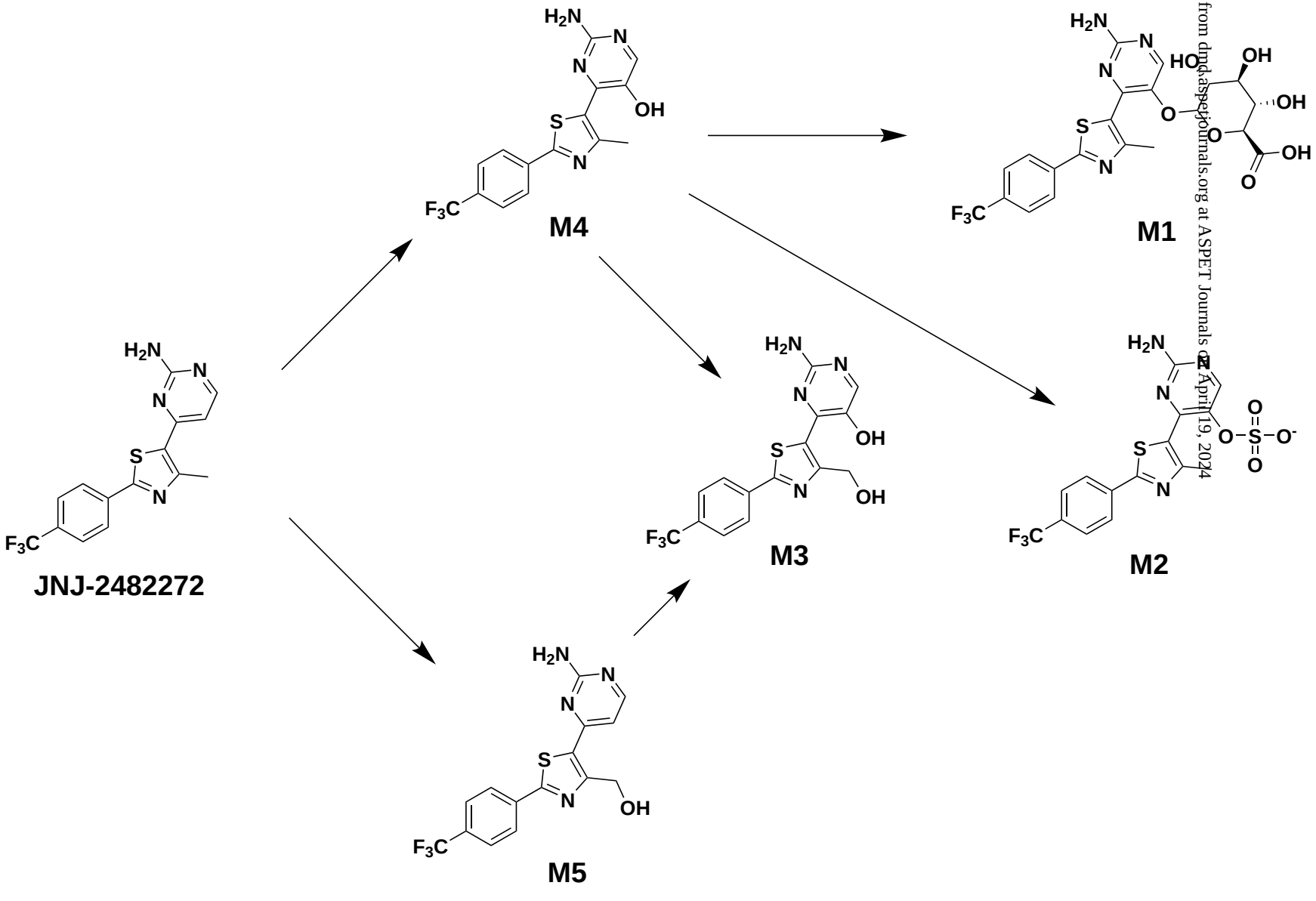

Scheme 1